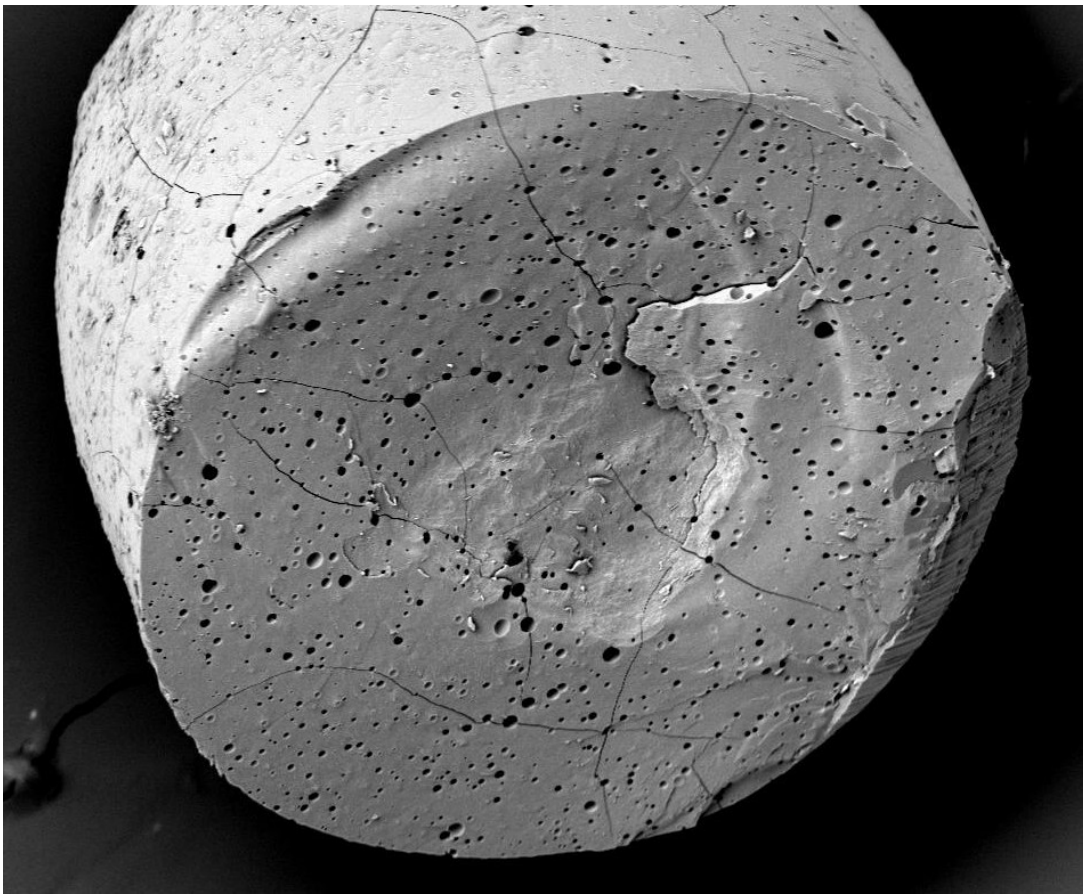


# CHALMERS



## Pellets formulation of crystalline nanoparticles A formulation process and characterization study

*Master of Science Thesis*

**PATRIK G TRÄFF**

Department of Chemical and Biological Engineering  
Division of Applied Chemistry  
CHALMERS UNIVERSITY OF TECHNOLOGY  
Göteborg, Sweden, 2011



# Pellets formulation of crystalline nanoparticles

A formulation process and characterization study

PATRIK G TRÄFF

SUPERVISORS:

Katrin Walter, AstraZeneca

Johan Gadd, AstraZeneca

Johan Hjærtstam, AstraZeneca

EXAMINER:

Krister Holmberg, Chalmers University of Technology

Department of Chemical and Biological Engineering  
CHALMERS UNIVERSITY OF TECHNOLOGY  
Göteborg, Sweden 2011

# Pellets formulation of crystalline nanoparticles

A formulation process and characterization study

PATRIK G TRÄFF

© PATRIK G TRÄFF, 2011.

Department of Chemical and Biological Engineering

Applied Chemistry

Chalmers University of Technology

SE 412 96 Göteborg

Sweden

Telephone +46 (0)31 772 10 00

The work was carried out at:

AstraZeneca R&D Mölndal

Pepparedsleden 1

SE-431 83 Mölndal

Telephone +46 (0)31 776 10 00

[www.astrazeneca.se](http://www.astrazeneca.se)

Cover: A cleaved pellet of API and trehalose coating.

Pellets formulation of crystalline nanoparticles  
A formulation process and characterization study

PATRIK G TRÄFF

Department of Chemical and Biological Engineering  
Chalmers University of Technology

## **Abstract**

A large proportion of new drug compounds in the pharmaceutical industry have an exceptionally low solubility in water which might cause poor bioavailability. This has become an increasing problem within formulation development, leading to abandoned development efforts. One solution to this problem could be to formulate the poorly soluble drugs into crystalline nanosuspensions. This step requires a process where the drug nanoparticles are embedded in a fast dissolving coating substrate, such as sugar, and spray coated onto microcrystalline cores in a fluidized bed. The coating substrate must be able to prevent agglomeration of the drug nanoparticles during the coating process and at the redispersion of the particles. The processability depends on the stickiness of the coating substrate. It is crucial that the coating substrate redisperses immediately and thus releases the nanoparticles, when in contact with water or gastrointestinal fluids. It is also important that the drug nanoparticles redisperse in the same particle size in relation to the bioavailability.

The coating substrate, excipients, composition of the nanosuspension and the process parameters were evaluated. Trehalose was shown to be the most favorable coating substrate, probably due to its high T<sub>g</sub>. It was able to prevent agglomeration of the crystalline drug nanoparticles during the coating process. The redispersion was shown to be rapid and the nanoparticles were redispersed in the same size as before the coating process.

The drug load was increased from 10% API to 30% API in the nanosuspension, thus a drug nanosuspension that could shorten the coating process was obtained.

The inlet airflow was shown to be the most critical parameter to obtain a well working process. High airflow provided a better non-sticky process but this parameter was limited by the equipment capability. The drying capacity can be calculated from the moisture content and airflow. This can give insight of how the fluidized bed behaves when coating sticky substances such as sugar.

Keywords: Fluid bed, nanoparticles, nanosuspension, pellet coating, poorly soluble

## **Acknowledgements**

First and foremost I would like to thank my head supervisor Katrin Walter for all the time that she has dedicated to my project.

Thanks to Johan Gadd for helping me with the wet milling and support during the project.

Johan Hjærtstam, thanks for valuable inputs during the project and for introducing me to Norberg.

Mats O Johansson. Thanks for helping me with considerations in the coating process and the calculations of the moisture contents.

Thanks to Olof Svensson & Anders Sparén for helping me with Raman spectroscopy and to interpret the results.

Thanks to Lennart Lindfors for interesting and valuable discussions during the project.

Caroline Wingolf, thanks for the help with wet milling procedures.

Thanks to the people at Formulation Science and Medicines Evaluation within AstraZeneca, Mölndal for making me feel welcome and a part of the team.

Thanks to my examiner, Krister Holmberg for support and patience during the project.

## **Glossary**

**Absorption site** - Sites in the body where drugs can be absorbed.

**API** - Active pharmaceutical ingredient.

**Bioavailability** - A measure of the rate and extent of drug absorption from an administered dose, which is expressed as a ratio to an intravenously administered dose or a commercial drug.

**Core** - Charged material as MCC/sugar cores in a fluid bed coater.

**Diffusion** - The spread of particles from regions of higher concentration to regions of lower concentration.

**Disaccharide** - Substance which is composed of two linked simple sugars (see saccharides).

**Dosage form** - Pill, tablets, capsules, drinks etc. are commonly used forms of drugs or medication intended for administration or consumption.

**Gastrointestinal** - The gastrointestinal tract refers to the stomach and intestine.

**Intravenous injection** - An introduction of a substance into a vein by the use of a needle.

**Micronized particles** - Solid particles which have had a reduction in size to the micrometer scale.

**Mollierdiagram** - A graphic tool of the relations between air temperature, humidity, enthalpies and more.

**Peak plasma concentration** - Change in plasma concentration over time.

**Pellets** - Discharged material of the fluid bed coater, consisting of core and coating substrate.

**Radius of gyration** - A tool to describe the dimensions of a polymer.

**Redisperse** - The term used when the pellets redisperse and thus releases the nanoparticles into the water or gastrointestinal fluid.

**Saccharide** - A carbohydrate, which is an organic compound consisting of carbon, hydrogen and oxygen. Saccharides and disaccharides are commonly referred to as sugars.

**Saturation solubility** - The concentration of a certain substance when the solvent becomes saturated.

**Slurry** - Refers to the solution containing stabilizers and API before the wet milling procedure.

**Spray drying** - When the suspension in a fluidized bed dries before colliding with pellets.

**Static diffusion layer** - A layer on the drug particles where  $h$  is the thickness in the Noyes-Whitney equation.

**STP** - Standard temperature and pressure, standard conditions for experimental measurements to allow comparisons between different sets of data,  $0^\circ$  and  $0.986\text{atm}$ .

**Systemic circulation** - System which carries oxygenated blood from the heart and brings back deoxygenated blood to the heart. The systemic circulation is part of the cardiovascular system.

**Weight average molecular weight** - A way of describing the molecular weight of a polymer.

## Table of contents

|          |   |           |
|----------|---|-----------|
| <b>1</b> | <b>Introduction.....</b>                                      | <b>1</b>  |
| 1.1      | Background.....   | 1         |
| 1.2      | Objective.....  | 1         |
| 1.3      | Scope.....  | 2         |
| <b>2</b> | <b>Theory.....</b>  | <b>3</b>  |
| 2.1      | Bioavailability.....  | 3         |
| 2.1.1    | Absolute bioavailability.....                                 | 3         |
| 2.1.2    | Relative bioavailability.....                                 | 4         |
| 2.2      | Suspensions and solid dispersions.....                        | 4         |
| 2.3      | Nanosuspensions.....  | 4         |
| 2.3.1    | Stabilizing a nanosuspension.....                             | 5         |
| 2.3.2    | Manufacturing nanosuspensions with wet milling technique..... | 5         |
| 2.4      | Glass transition temperature.....                             | 6         |
| 2.5      | Amorphous versus crystalline solid state properties.....      | 6         |
| 2.6      | Solid dosage formulation.....                                 | 7         |
| 2.7      | Coating process in fluidized beds.....                        | 7         |
| 2.8      | Process parameters.....                                       | 9         |
| 2.9      | Inputs and response in the coating process.....               | 9         |
| <b>3</b> | <b>Materials and Methods.....</b>                             | <b>11</b> |
| 3.1      | Materials.....  | 11        |
| 3.1.1    | Felodipine.....   | 11        |
| 3.1.2    | PVP K30.....  | 11        |
| 3.1.3    | AOT (docusate sodium).....                                    | 12        |
| 3.1.4    | Sugars.....   | 12        |
| 3.1.4.1  | Sucrose.....  | 12        |
| 3.1.4.2  | Trehalose.....  | 13        |
| 3.1.4.3  | Mannitol.....   | 13        |
| 3.1.5    | Microcrystalline cellulose cores.....                         | 13        |
| 3.2      | Methods.....  | 14        |
| 3.2.1    | Preparation of the suspensions.....                           | 14        |
| 3.2.2    | Micrometer to nanometer with wet milling technique.....       | 14        |
| 3.2.3    | Lab fluidized bed coater.....                                 | 14        |
| 3.2.4    | Scale up coating.....   | 16        |

|          |  |           |
|----------|--|-----------|
| 3.2.5    | Redispersion.....  | 16        |
| 3.2.6    | Beadcheck analyzer .....   | 17        |
| 3.2.7    | Scanning electron microscopy .....                                 | 17        |
| 3.2.8    | Particle size distributions of nanosuspensions.....                | 17        |
| 3.2.9    | Particle size distribution for redispersed particles .....         | 18        |
| 3.2.10   | Raman spectroscopy .....   | 18        |
| <b>4</b> | <b>Results and Discussion .....</b>                                | <b>19</b> |
| 4.1      | Particle size of the milled suspensions.....                       | 19        |
| 4.2      | Ratio of API nanoparticles and coating substrate .....             | 19        |
| 4.3      | Processability for different coating substrates .....              | 20        |
| 4.4      | Mean particle size of redispersed nanoparticles .....              | 21        |
| 4.5      | Amorphous or crystalline coating substrate.....                    | 22        |
| 4.6      | Composition and drug load of the nanosuspensions.....              | 24        |
| 4.7      | Determination of coating layer thickness .....                     | 25        |
| 4.8      | Optimization of the process parameters.....                        | 26        |
| 4.9      | Coating with increased airflow and increased temperature out ..... | 26        |
| 4.10     | Visual redispersion with light microscopy .....                    | 29        |
| 4.11     | Scale up.....  | 30        |
| 4.12     | Quality of the pellets uniformity.....                             | 31        |
| <b>5</b> | <b>Conclusions.....</b>  | <b>33</b> |
| <b>6</b> | <b>Future work.....</b>  | <b>35</b> |
| <b>7</b> | <b>References.....</b>   | <b>37</b> |
|          | <b>Appendix .....</b>  | <b>41</b> |

# 1 Introduction

## 1.1 Background

Today, a very large proportion of new drug candidates have an exceptionally poor solubility in water [1]. This has become an increasing problem within the pharmaceutical industry in terms of obtaining sufficient dissolution within the gastrointestinal tract, which is necessary for adequate bioavailability [2]. This problem can be addressed by formulating the drugs into crystalline nanosuspensions. The reduced particle size allows for increased dissolution rates and thus enhanced bioavailability [3]. The nanosuspensions are preferably converted to solid dosage forms for oral absorption from a marketing and physical point of view, them being patient compliance and stability of the nanoparticles respectively [4]. Spray coating in a fluidized bed is one way of drying the nanoparticles, as the solvent is evaporated. This step can though create thermal stress on the particles which can lead to aggregation [3]. By using an inert core on which the drug particles can adhere one can decrease the agglomeration and with the help of stabilizers, increase the wetting, which is also essential.

When redispersing the drug nanoparticles they should disperse as nanosuspensions and thus attain its original nanoparticle size when in contact with water or gastrointestinal fluids, giving good dissolution rates. Since the pellets studied are made for immediate release, rapid redispersion of the nanoparticles is a requirement. This rapid dissolution can be achieved by using easily disintegrating sugars as coating substrate. However, the sugars low  $T_g$  and its hygroscopicity can cause challenges like stickiness or cohesiveness [5]. Nanosuspensions of drugs can help formulation scientists to successfully formulate dosage forms of compounds which have significantly low solubility. Emulsions and liposomes can also be used to solve these problems when the compound is poorly soluble in water but soluble in oil. But nanosuspensions are the only choice when the compound is poorly soluble in both water and oil, which would otherwise lead to abandoned development efforts [1].

## 1.2 Objective

The aim of this thesis was to find a suitable coating substrate and excipients for a crystalline active pharmaceutical ingredient (API) nanosuspension in order that the drug nanoparticles regain their original particle size when redispersed. The manufacturing process where the nanosuspension is spray coated onto spherical microcrystalline cellulose (MCC) cores must also be effective, since the coating substrates tend to complicate the process conditions by their stickiness.

There are two basic requirements that must be fulfilled:

- 1) The spray rate of the suspension to the fluid bed, which is an indication of the processability, must be adequate. A suitable coating substrate that can give sufficient spray rate and thus good processability must be found since this is directly associated to the process time and thus production costs.
- 2) When redispersing the drug nanoparticles after spray coating, they must be redispersed to their original nanoparticle size.

### **1.3 Scope**

Since the project reaches over several scientific fields such as; biopharmacy, surface chemistry, process technology and nanotechnology it is important to specify limitations within the project. Fluidized beds have been the object for many other projects before [6, 7, 8]. This is why focus will not be on optimizing process parameters in fluidized beds but more on the compositions of the suspension in order to obtain a process with sufficient processability, which can be optimized further in future works.

## 2 Theory

### 2.1 Bioavailability

The term bioavailability is often used in pharmacology and an explanation is essential for understanding the importance of the expression.

#### 2.1.1 Absolute bioavailability

Absolute bioavailability can be calculated when comparing the total amount of drug that reaches the systemic circulation from an intravenous injection, with the total amount of the same drug administered via another route. The dose administered intravenously is used as reference since it is introduced directly into the systemic circulation, thus giving 100% bioavailability. By using a plasma concentration-time curve, the absolute bioavailability can be calculated with the help of equation 2.1.

$$\text{Absolute bioavailability} = (\text{AUC}_T)_{\text{abs}} \times D_{\text{iv}} / (\text{AUC}_T)_{\text{iv}} \times D_{\text{abs}} \quad (\text{eq. 2.1})$$

Here,  $(\text{AUC}_T)_{\text{abs}}$  is the total area under the plasma concentration-time curve from the dose of the drug administered via an absorption site.  $(\text{AUC}_T)_{\text{iv}}$  is the total area under the curve following intravenous injection of the drug.  $D_{\text{iv}}$  is the size of the single dose of drug administered intravenously and  $D_{\text{abs}}$  is the size of the drug administered via absorption site (see fig. 2.1) [2].

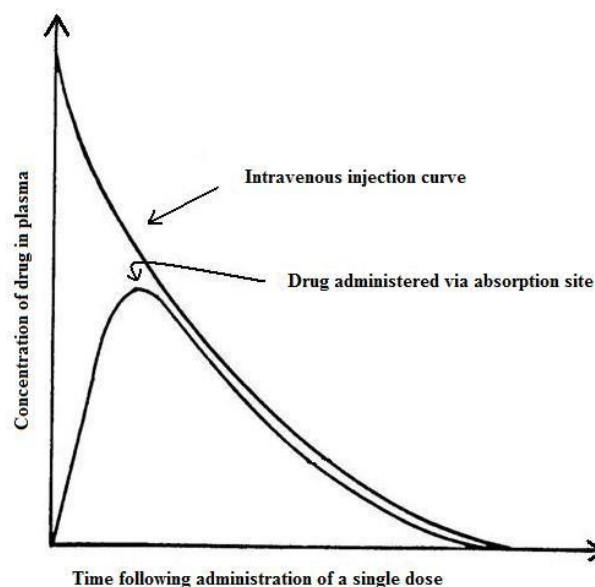


**Figure 2.1.** Typical plasma concentration-time curves from administering equivalent doses of the same drug by different routes.

### 2.1.2 Relative bioavailability

The relative bioavailability can be determined when the drug cannot be administered by an intravenous injection. Instead of using the intravenous injection as a reference, a standard oral dosage form is used. This can be either an orally administered solution or an established commercial preparation that has been proven to be clinically effective. This standard oral reference is compared with a test oral dosage form of the same drug. A similar equation as for the absolute bioavailability gives the relative bioavailability from a plasma concentration-time curve.  $(AUC_T)_{\text{test}}$  and  $(AUC_T)_{\text{standard}}$  are the total areas under the plasma concentration-time curve of the test and standard dosage forms respectively.  $D_{\text{test}}$  and  $D_{\text{standard}}$  is the size of the single doses of the both dosage forms. The equation is similar to the equation for absolute bioavailability [2]:

$$\text{Relative bioavailability} = (AUC_T)_{\text{test}} \times D_{\text{standard}} / (AUC_T)_{\text{standard}} \times D_{\text{test}} \quad (\text{eq. 2.2})$$

## 2.2 Suspensions and solid dispersions

The terms suspension and solid dispersion are frequently used to describe systems in the pharmaceutical industry, why a definition of both terms are suitable. A pharmaceutical suspension refers to insoluble particles, preferably greater than 1  $\mu\text{m}$  in diameter, dispersed in an aqueous liquid medium [2]. Solid dispersions in the pharmaceutical industry refers to a two or more component system where the drug is dispersed preferably as small particles in a hydrophilic matrix in the solid state [9].

## 2.3 Nanosuspensions

A nanosuspension is a submicron colloidal dispersion of particles which are stabilized by suitable surfactants [10]. In pharmaceutical industry the drug is in the nanosize, typically between 100 – 200 nm, enabled by recent advances in milling technology [11], giving the API increased surface area. This increase in surface area gives the nanoparticles an increased dissolution rate and higher saturation solubility in comparison with micronized drugs. This leads to higher bioavailability of drugs administered as nanosuspensions [12]. This can be correlated to the Noyes-Whitney equation:

$$dM/dt = DA(C_s - C)/h \quad (\text{eq. 2.3})$$

Where  $dM/dt$ =rate of dissolution,  $D$ =diffusion coefficient of the drug in solution,  $A$ =effective surface area of the drug,  $C_s$ =saturation solubility of the drug,  $C$ =concentration of the drug in the bulk fluid,  $h$ =thickness of the static diffusion layer. Therefore, as the particle size of the drug decreases, the surface area increases thus leading to improved dissolution rates. However, if the nanoparticles form aggregates upon redispersion, the overall surface area would decrease and the dissolution rate would as a consequence also decrease, giving lower bioavailability [2, 3, 11]. In addition, the dissolution rate can be further increased by the saturation solubility of the nanosized API explained by the Ostwald-Freundlich equation (eq. 2.4) [13].

$$(RT/V_m) \times \ln(S/S_0) = 2\gamma/r \quad (\text{eq. 2.4})$$

Here,  $S$  is the solubility of small particles of size  $r$ .  $S_0$  is the equilibrium solubility,  $R$  is the universal gas constant,  $T$  is the temperature,  $V_m$  is the molar volume and  $\gamma$  is the surface tension. Particles at the nanoscale should give increased saturation solubility from the Ostwald-Freundlich equation and thus enhanced dissolution rate according to the Noyes-Whitney equation.

### 2.3.1 Stabilizing a nanosuspension

When forming nanoparticles from larger particles, a new surface area is created which impose a Gibbs free energy cost associated with the formation of additional interface. The nanosuspensions created are thus thermodynamically unstable and will try to minimize their total energy by agglomerating [1, 4]. An efficient way of addressing this problem is by the addition of stabilizers. A nonionic polymer is used to coat the surface of the drug with its hydrophobic chain while the hydrophilic part can be projected into the water. Compression of the polymers causes loss of entropy and is therefore unfavorable [1]. This so called steric repulsion is often not enough for stabilizing a nanosuspension, since it can be sensitive to for example temperature fluctuations. Electrostatic stabilization can be enabled by adding an ionic surfactant. The electrostatic stabilization is based on the repulsive forces when the diffuse double layers surrounding the drug nanoparticles start to overlap. This gives an increase in ion concentration which is entropically unfavorable [14]. The nonionic polymer and the ionic surfactant work well together, it permits greater coverage of the charged surfactant. This occurs because the self-repulsion of the ionic surfactant is minimized by the polymer which permits closer packing [1]. The amount of stabilizers added must be in the right weight ratio. Excess stabilizers promotes Ostwald Ripening, which is a process where the difference in solubility with particle size leads to material from smaller particles going to larger particles and thus induce particle growth with time [15, 16]. Insufficient amount of stabilizers added leads to agglomeration or aggregation [16].

### 2.3.2 Manufacturing nanosuspensions with wet milling technique

The most common way of manufacturing nanosuspensions is by the so called top-down techniques. This means starting from a large sized powder and performing a size reduction instead of building up to nanoscale (bottom-up technique) [17]. There are different technologies for this but the most used today is wet milling where the milling chambers are charged with milling media, drug, stabilizers and water [16]. The milling media is typically highly crosslinked polystyrene balls, zirconia- or glass beads. The milling technique has several advantages; it is a simple technology, a low cost process and easy to scale up if a batch process is relevant. Disadvantages could be; potential erosion from milling media, potential growth of germs in water phase if there are long milling times and that the separation procedure of milling media costs time and money [17]. Crystalline nanosuspensions have been prepared by wet milling techniques at

AstraZeneca Södertälje and are used in this master thesis. Additional nanosuspensions of different volumes and composition were made according to the wet milling procedure.

## 2.4 Glass transition temperature

The glass transition temperature,  $T_g$ , is most likely the most important property of an amorphous material [18, 19]. When an amorphous sample is heated above its  $T_g$  several properties of the sample changes due to increased molecular mobility and the amorphous solid changes from being in a glassy state to a rubbery state. The increased mobility affects the samples properties such as volume, heat capacity, viscosity and dielectric relaxation [19]. The molecules are more stiff and brittle in the glassy state while they become more soft and flexible in the rubbery state.

The processability of amorphous materials is often problematic since they become more elastic and sticky above their  $T_g$ . Water is often used as solvent which acts as an additional plasticizer for the amorphous material and thus decreases the  $T_g$  and make it even harder to process because of its stickiness or cohesiveness. The decrease in  $T_g$  can be significant even at very small water amounts [5, 18] This can be theoretically calculated by the use of the Gordon-Taylor equation:

$$T_{g_{mix}} = (w_1 T_{g1} + K w_2 T_{g2}) / (w_1 + K w_2) \quad (\text{eq. 2.5})$$

$$K = \rho_1 T_{g1} / \rho_2 T_{g2} \quad (\text{eq. 2.6})$$

Where  $w$  corresponds to the weight fraction of the amorphous material in the equations above and  $T_g$  for the glass transition temperatures.  $K$  is a constant which can be calculated by the Simha-Boyer rule in equation 2.6. The trials 1 and 2 in the equations represent the amorphous compounds with the lowest and highest glass transitions temperatures respectively [20].

## 2.5 Amorphous versus crystalline solid state properties

The main advantage concerning amorphous drugs in the pharmaceutical industry is that the lack of order in the crystal lattice of amorphous solids requires less energy and thus gives maximal solubility advantage in comparison to the crystalline form of the drug and thus greater bioavailability. However, because of the higher potential energy the amorphous solids are more physically unstable and they are prone to crystallize and degrade [19]. Understandable, there are significantly more hurdles to overcome for amorphous drugs than for crystalline in the formulation of new drugs intended for the international market [2, 21].

Crystalline drugs as nanosuspensions provide greater stability and are most often preferred during pharmaceutical development [22].

The solid state form of the excipients in a solid dosage form can also be crucial for the effects of the drug.

## 2.6 Solid dosage formulation

In this work pellets have been chosen as dosage form for the crystalline nanosuspensions due to its many advantages for the administration of oral controlled release dosage forms; they disperse freely in the gastrointestinal tract and thus maximize drug absorption, reduce peak plasma concentrations and minimize side effects. High local concentrations are avoided and the processing can be made more flexible by coating the pellets with different drug substances or different drug loads [23]. The advantage with a higher drug load is that different sizes of capsules can be filled with the same pellet formulation to obtain a variety of doses.

The structure of a pellet is an inert core and a layer containing coating substrate and nanoparticles (see fig. 2.2). The core can be spherical particles in the 300–1500  $\mu\text{m}$  range and consist of sugar or microcrystalline cellulose (MCC).

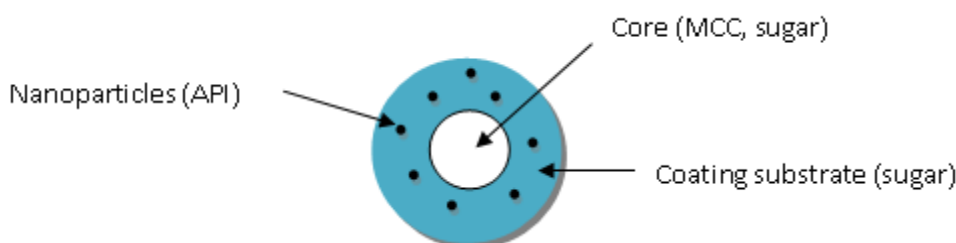


**Figure 2.2.** Schematic drawing of a pellet consisting of core, nanoparticles and coating substrate.

## 2.7 Coating process in fluidized beds

Coating is an important process in the pharmaceutical industry as well as in the agricultural, food and chemical industry. In the pharmaceutical industry, the coating equipment can be divided into four main types namely; pan coating, top-spray fluidized bed coating, rotor coating with tangential spray and Wurster bed coating (bottom spray) [24]. Here, the Wurster or bottom-spray coating equipment is used. It consists of an expansion chamber, an annulus, a Wurster tube, a distributor plate and a spray nozzle (see fig. 2.3).

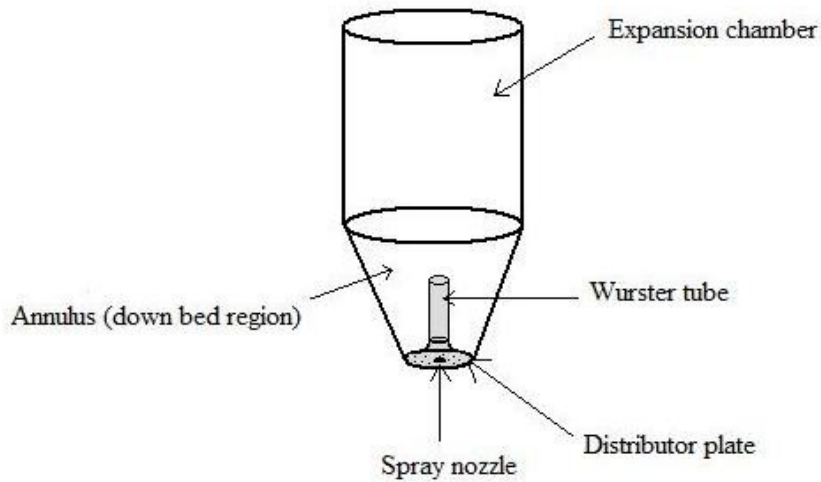


**Figure 2.3.** Schematic drawing of a Wurster type bed with main components.

The coating process consists of air supporting the pellets in a vertical column with an upwardly moving stream. The suspension is atomized onto the suspended pellets according to figure 2.4 [25]. The gas flow accelerating the pellets comes from both the fluidization air as well as the spray nozzle flow which forms a mist of the suspension or solution [24, 26]. The droplet size is determined by the atomizer air pressure and the droplets should be small enough to obtain a smooth coating but not so small so that they run the risk of drying out before being deposited on the pellets [24]. When the pellets get hit by the suspension droplets and move upwards the column they get to a region which is called the fountain region. Here the coated pellets fall back to the sides by the gravitational force (see fig. 2.4). The pellets must dry before entering this region to avoid agglomeration.

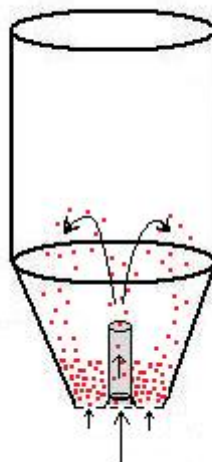


**Figure 2.4.** Schematic drawing of a Wurster type bed with pellets (red dots) during air flow.

## 2.8 Process parameters

To obtain a uniform layer of the suspension on the pellets, several key process parameters must be considered. The key parameters and their main impact on the process are summarized in table 2.1.

**Table 2.1.** *Key process parameters and their main impact on the coating process.*

| <i>Parameter</i>           | <i>Impact</i>                                   |
|----------------------------|---|
| Spray rate of suspension   | Agglomeration, process time                     |
| Atomizing airflow          | Droplet size, spray drying, aggro., yield       |
| Inlet air temperature      | Agglomeration, spray drying, yield              |
| Bed temperature            | Agglomeration, spray drying, yield              |
| Inlet airflow              | Overwetting, pellets in filter, drying capacity |
| Inlet air moisture content | Drying capacity, overwetting                    |

Maximum spray rate is limited by viscosity and tackiness of the coating liquid, the drying capacity and droplet size of the fluidized bed system also limits the spray rate. Exceeding spray rate can result in irreversible agglomeration due to lower bed temperature because more liquid is pumped in which cools the system [24, 27]. Atomization air pressure is an important parameter to control the droplet size distribution and velocity. Spray drying occurs when an excessive amount of atomization air pressure is used while agglomeration occurs at insufficient amount of atomization pressure. The temperature needs to be adjusted properly for each individual coating session. An elevated inlet air temperature ( $T_{in}$ ) can lead to agglomeration due to softening of the coat but a sufficient temperature is needed to evaporate the solvent. The inlet air flow determines the particle flow in the bed. Too high air volume results in pellets getting trapped in the filter in the upper part of the bed. If the air flow is not sufficient, the pellets get overwetted. A higher spray rate can be obtained when the inlet moisture content is low, otherwise spray drying may occur. At higher inlet air humidities there is a risk of overwetting and it is also difficult to remove residual moisture in the coat at higher inlet air moisture contents. The inlet air humidity is indicated by the dew point temperature. At this temperature, the air is saturated with moisture. The dew point temperature can be held constant, providing reproducible drying rates and better film properties [27]. These key parameters are related and must be taken into account when designing a process to obtain a high quality coating [24].

## 2.9 Inputs and response in the coating process

The amount of excipients and drug in the nanosuspension determines how much water that has to be evaporated in the fluidized bed. It is important that the spray rate is sufficiently high because this determines the overall process time. A higher amount of API in the nanosuspension gives a higher drug load and thus more API can be applied under shorter time with the same spray rate. This could be beneficial from an economical point of view. The processability is measured by the product- and coating yield, the degree of agglomeration and the overall process time.



### 3 Materials and Methods

#### 3.1 Materials

##### 3.1.1 Felodipine

The substance used, ethyl methyl 4-(2,3-dichlorophenyl)-1,4-dihydro-2,6-dimethyl-3,5-pyridinedicarboxylate (Felodipine), was provided by AstraZeneca R&D Mölndal. It has a melting point temperature of about 145°C and a log P value at approximately 4, indicating its high lipophilicity [28]. The drug is a calcium channel blocker. It relaxes the blood vessels which makes it easier for the heart to pump [29]. Felodipine is referred to as the API in this thesis.

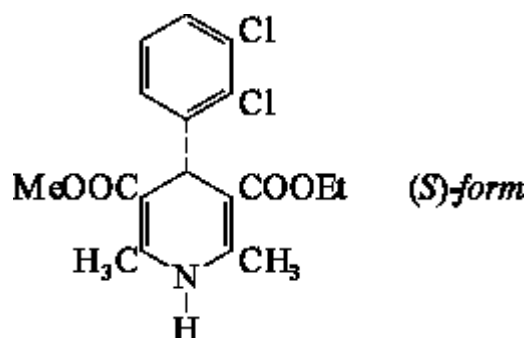


**Figure 3.1.** The *(S)*-form of Felodipine [28].

##### 3.1.2 PVP K30

Polyvinylpyrrolidone is a hydrophilic polymer often used in the food and pharmaceutical industry. There are many different sorts of PVP depending on the degree of polymerization denoted by the K value in the name. PVP K30 has a molecular weight of approximately  $4\text{-}5 \times 10^4$  g/mol [30]. PVP K30 acts as a steric stabilizer in the nanosuspension. It was obtained from BASF, Ludwigshafen Germany. In this thesis, PVP K30 was also evaluated as a coating substrate.

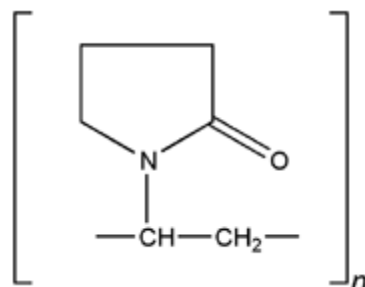


**Figure 3.2.** A monomeric unit of PVP [30].

### 3.1.3 AOT (docusate sodium)

The anionic surfactant used to provide electrostatic stabilization in the nanosuspension was obtained from Sigma-Aldrich St. Louis, USA. AOT is hygroscopic with a melting point of approximately 155°C and has been widely used in pharmaceutical formulations.

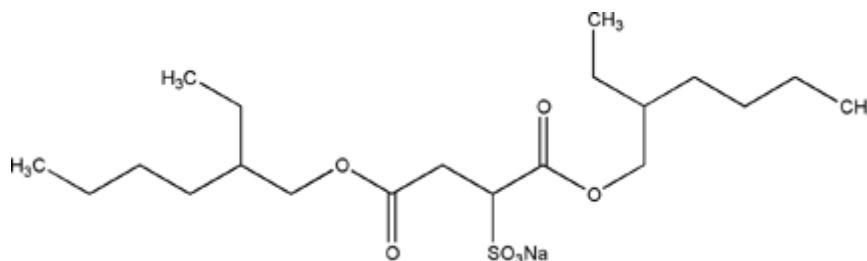


**Figure 3.3.** Schematic image of the structural formula of AOT [30].

### 3.1.4 Sugars

The coating substrate is typically sugars or water soluble polymers [4, 31]. One major problem with sugars is their stickiness during the spray coating step. Myo-inositol, lactose, fructose and glucose were also evaluated and are presented in appendix A.

#### 3.1.4.1 Sucrose

Sucrose is widely used in the pharmaceutical industry [4, 32]. Sucrose is a disaccharide with a Tg of approximately 60°C, it is hygroscopic and absorbs up to 1% water [30, 33]. Sucrose was obtained from Sigma Chemical CO. St. Louis, USA.

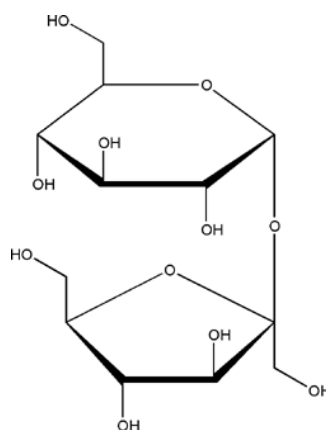


**Figure 3.4.** The chemical structure of sucrose [30].

### 3.1.4.2 Trehalose

Trehalose is a disaccharide with a moisture content of approximately 9.5% [30]. It has a Tg of approximately 107°C which is relatively high for a water soluble sugar [33]. Trehalose has not been as widely used as sucrose for spray drying applications [4]. It was obtained from Asahi Kasei Fine Chem Co Ltd. Osaka, Japan.

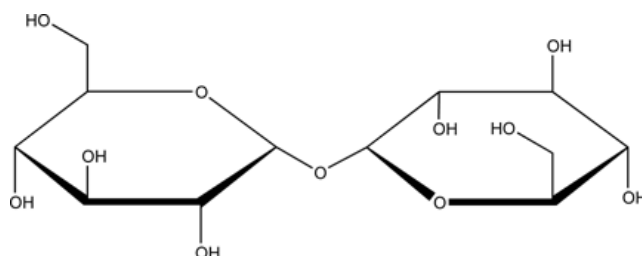


**Figure 3.5.** *The chemical structure of trehalose [30].*

### 3.1.4.3 Mannitol

Mannitol is a sugar alcohol which is widely used in the pharmaceutical and food industry. It is, unlike sucrose and trehalose, not hygroscopic and the chemical structure is linear unlike the disaccharides (see fig. 3.6) [30]. It has a Tg of approximately 87°C and has been used widely for spray- and freeze drying of nanoparticles [4]. It was obtained from Merck KGaA, Germany.

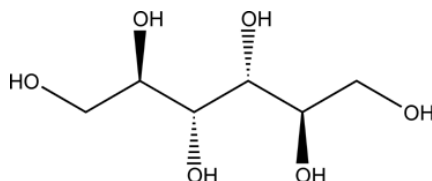


**Figure 3.6.** *The chemical structure of mannitol [30].*

### 3.1.5 Microcrystalline cellulose cores

Cores of 300–500  $\mu\text{m}$  in diameter (CP305) were chosen for all experiments. These cores do not dissolve in water and provides a surface for the nanosuspension coating to be applied. They were obtained from FMC Corporation New Jersey, USA.

## 3.2 Methods

### 3.2.1 Preparation of the suspensions

A stabilizer solution was made at room temperature by adding PVP K30 and AOT to Milli-Q water to obtain a composition of 1.3% (w/w) PVP K30 and 0.067% (w/w) AOT. This stabilizer solution was mixed well with a magnetic stirrer.

The API was added to the stabilizer solution to a concentration of 10% (w/w) API. Mixing was done by magnetic stirring and ultrabath.

A 30% (w/w) API suspension was also prepared with the same procedure as the 10% (w/w) API. The stabilizer composition was multiplied by three giving a stabilizer composition of 3.9% (w/w) PVP K30 and 0.201% (w/w) AOT.

### 3.2.2 Micrometer to nanometer with wet milling technique

Milling suspension volumes of 1-30 ml in each vessel where two vessels can be milled at the same time thus giving a suspension of maximum 60 ml can be done in the Planetary Micromill Pulverisette 7 Premium Line from Fritsch GmbH, Germany. Vessels of 20, 45 or 80 ml can be used where the grinding media is zirconiabeads of 0.6-0.8 mm. The Fritsch Micromill does not have a cooling system and its maximum rotation speed is 800 rpm.

The prepared slurry was milled for 3x30 minutes at 700 rpm in two 80 ml vessels before it was taken out by syringe to obtain a 63 g crystalline API nanosuspension.

The Dynamill Multilab from CB mills is used for larger volumes where the grinding chamber used here was 150 ml and a continuous or batchwise configuration could be chosen. The bead mill has an operating speed of 5000 rpm with a water cooling system. The grinding media used at AstraZeneca is soda lime glass beads 0.4-0.6 mm obtained from Mo-Sci Missouri, USA.

A continuous configuration was chosen when 1000 ml slurry was milled for 160 minutes at approximately 2870 rpm in the Dynamill, giving a crystalline nanosuspension of API.

### 3.2.3 Lab fluidized bed coater

Small scale spray coating was carried out with lab fluidized bed coater (Instrumentverkstad, AstraZeneca Mölndal) with a batchsize of 5-50 g to obtain a well working process before scaling up. With this coater, no Wurster tube was needed to distribute the cores during the process since there is only a small amount in this scale. The coater is equipped with a 2 inch distributor plate and a 0.8 mm Schlick nozzle. The process parameters was preset as follows; atomizer pressure 1 bar, airflow was set to 10 Nm<sup>3</sup>/h, the inlet temperature, 70°-75° and the exhaust air temperature from the bed (T<sub>out</sub>) was held between 42°-48°.

The spray rate was determined by the stickiness of the sprayed sugar. A high spray rate indicated good processability. When a functional composition of excipients and API had been prepared that had acceptable processability and that, when redispersed, had an acceptable particle size, then the parameters could be changed to optimize the process.

Coating substrate was added to the nanosuspensions before the coating process could start. The ratio between the coating substrate and the API was set to 1:1 but other ratios were also evaluated. Additional stabilizers were also added together with the coating substrate (2% (w/w) PVP K30 and 0.07% (w/w) AOT).

Crystalline nanosuspensions of different compositions were pumped from a beaker into the bottom of the bed through the spray nozzle where it was atomized out into the column. The microcrystalline cores were suspended in the column by the fluidization air through the distributor plate and also by the air from the nozzle, before the suspension was pumped in. The amount of cores charged was typically 12 g when a nanosuspension of 60 g was sprayed.

The product yield and the coating yield were calculated after each spray coating process (see equation 3.1 and 3.2). Here T=core material (charged weight), F=theoretical coat (charged weight) and A=actual weight (product weight).

$$\% \text{ Actual yield (product yield)} = A / (T + F) \times 100 \quad (\text{eq. 3.1})$$

$$\% \text{ Coating yield} = (A - T) / F \times 100 \quad (\text{eq. 3.2})$$



**Figure 3.7.** *The lab fluidized bed coater.*

### 3.2.4 Scale up coating

Scale up in fluidized beds can be calculated based on geometrical considerations, but the optimization is often based on trial and error methods [34]. By dividing the upscaled air distributor plate diameter ( $A_2$ ) with the lab scale distributor plate area ( $A_1$ ) squared, an upscale value is obtained ( $W$ ). By multiplying this value with the lab scale spray rate or airflow, the spray rate or inlet airflow for the upscaled process is obtained.  $(A_2/A_1)^2 = W$ ,  $W \times S_1 = S_2$ .

Other methods used for scale up in fluidized beds are shown below (eq. 3.3 and 3.4).

$$S_2 = S_1 \times V_2/V_1 \quad (\text{eq. 3.3})$$

$$S_2 = S_1 \times A_2/A_1 \quad (\text{eq. 3.4})$$

Here,  $S_1$  is the spray rate in the lab scale equipment and  $S_2$  in the bigger scale of the fluidized bed.  $V_1$  is the volume of inlet airflow in lab scale and  $V_2$  the volume of inlet airflow entering the scaled up fluid bed.  $A_1$  and  $A_2$  are the air distributor plate areas for the lab scale equipment and the bigger scale fluidized bed respectively. [22].

The fluidized bed used for scale up tries in this thesis was Gandalf 3 which is an in house built fluidized bed with an air distributor plate of 4 inch. The amount of discharged pellets can be in the range of 100-700 g. The amount of charged cores used was 100 g for each trial.

### 3.2.5 Redispersión

It is important that the pellets redisperse immediately when in contact with water or intestinal fluids. Coating substrates of sugar ought to redisperse rapidly enough where other hydrophilic coating substrates may not. This was evaluated by taking snapshots of single coated pellets when phosphate buffer (pH 6.8) came in contact with the coating. Using the software Image Pro Plus 5.1, resolution, time for snapshots and other parameters could be adjusted. This gave a good estimation of the redispersion rate of the nanoparticles. The visual effect was enhanced by the fact that the API nanosuspensions appeared milky white. The different colors in the picture for PVP K30 are due to the settings of light and exposure time in Image Pro Plus 5.1 (fig. 4.7).

### 3.2.6 Beadcheck analyzer

Pellet shape, thickness of the coating and distribution of pellet size with and without coating can be obtained using automated microscopy image analysis technique with the help of the software PharmaVision 830.

Uncoated microcrystalline cores are spread out over a glass slide and a camera takes pictures over the entire slide giving a size distribution curve and the mean diameter distribution by volume. The same procedure is done with coated pellets thus the coating thickness can be calculated and particle size distribution evaluated.

### 3.2.7 Scanning electron microscopy

Scanning electron microscopy (SEM) was used to visually determine the uniformity of the coating and worked as a quality measurement of the final pellets. It was also used to estimate the porosity of the sprayed films. The pellets were cleaved with a scalpel to get a surface that could be visualized in the SEM (Quanta 200, FEI, USA). The samples were first sputtered with gold (Cressington sputter coater 108 Auto, Cressington Scientific Instruments Ltd, England) in Argon environment for 100 s before analyzing them under high voltage (10kV) during scanning. The SEM produces images by hitting the samples with a high energy electron beam. The electrons interact with the atoms in the sample giving information about surface topography and other properties [35].

### 3.2.8 Particle size distributions of nanosuspensions

Light scattering is a very important tool for measuring particle size in colloidal solutions. The weight average molecular weight and the radius of gyration can be obtained from static light scattering while the Stokes radius can be obtained from dynamic light scattering [36].

Malvern Mastersizer 2000 uses static light scattering to confirm nanometer sized particles by measuring the amount of light scattered by a colloidal solution at different angles relative to the incident beam. The crystalline nanosuspensions were analyzed with this technique during and after the wet milling procedure to ensure that nanoparticles were obtained.

### 3.2.9 Particle size distribution for redispersed particles

FOQELS particle size analyzer uses dynamic or quasi-elastic light scattering, to determine the particle size of the crystalline API. This technique is more sensitive towards concentration and the condition of the sample.

When redispersing the nanoparticles, 7-8 mg of coated pellets was weighed in a 4 ml vial and 3 ml of water was added. After 30 minutes 1 ml was taken out from the vial and added to an empty 4 ml vial which was placed in the FOQELS particle size analyzer. A distribution curve was obtained after 2 minutes and every trial was repeated to ensure quality of the measurements.

### 3.2.10 Raman spectroscopy

Raman spectroscopy uses the vibrations of atoms when a sample is illuminated by a laser beam to provide essential information of the atoms and molecules in the solid. A photon excites a molecule from the ground state to a higher energy state and when the molecule relaxes back it emits a photon and returns to a different vibrational state. Here, Raman spectroscopy was used to determine phase transformations of the coated sugars but it can be used for a multitude of applications such as structure determination, order-disorder phenomena, adsorbed species and for identification of phases in a mixture [37].

The disaccharide trehalose and the sugar alcohol mannitol were evaluated based on their solid state form with Raman spectroscopy.

The powder form of the sugars, the sugars coated on microcrystalline cores and the coated sugar with API and stabilizers were examined to determine the phase transitions. MCC cores and MCC cores coated with sugar were used as reference samples.

## 4 Results and Discussion

### 4.1 Particle size of the milled suspensions

The particle size distribution was determined for all batches of crystalline API nanosuspension. Four batches were premade at AstraZeneca Södertälje, here called batches 1-4.

Batch 5 was milled in small scale to evaluate a composition with a higher solid amount and thus less water would be evaporated in the process.

Batch 6 was milled in larger scale in the Dynomill for scale up considerations. The particle size distribution was determined with static light scattering for all batches and the results are summarized in table 4.1 below. The particle size of batch 5 and 6 before the milling was 39  $\mu\text{m}$  and 43  $\mu\text{m}$  respectively. The larger mean particle size can be explained by the higher amounts of API and the larger scale of batch 6. All batches were in the expected and acceptable range (below 300nm).

**Table 4.1.** Mean diameter distribution by volume from static light scattering.

| <i>Batch</i> | <i>D[4,3]</i> | <i>Composition</i> | <i>Milled at</i> |
|--------------|---------------|--------------------|------------------|
| 1            | 200nm         | 10% API            | Södertälje       |
| 2            | 180nm         | 10% API            | Södertälje       |
| 3            | 150nm         | 10% API            | Södertälje       |
| 4            | 120nm         | 10% API            | Södertälje       |
| 5            | 240nm         | 30% API            | Möln dal         |
| 6            | 285nm         | 30% API            | Möln dal         |

### 4.2 Ratio of API nanoparticles and coating substrate

A ratio of 1:1 between the API and coating substrate has been the most widely used in earlier works [3, 31]. The ratio was examined with trehalose as coating substrate to give estimation if other ratios should be used. Trehalose was chosen as the coating substrate due to its high Tg of approximately 107°. Stabilizers (2% PVP K30 and 0.07% AOT) were added together with trehalose in trial 1-3 (see table 4.2) to further stabilize the nanoparticles since the stabilizer concentration was quite low comparing with earlier works to stabilize nanosuspensions [4]. Trial 4 was spray coated with the original nanosuspension (without trehalose or additional stabilizers). The results of the mean particle size before and after redispersion of the API nanoparticles are summarized in table 4.2.

It was shown that a ratio of 1:1 between the API and trehalose prevented agglomeration of the particles most effectively. Trial 3 gave an indication that additional stabilizers prevented some agglomeration of the nanoparticles when comparing with trial 4. The mean particle size is in an acceptable range in trial 1-3, but not in trial 4. This led to an additional spray coating trial with PVP K30 as the coating substrate.

**Table 4.2.** Mean particle size of different ratios of API and trehalose.

| <i>Trial</i> | <i>Ratio<br/>API:Trehalose</i> | <i>Mean particle size<br/>before spray drying<br/>(batch 1)</i> | <i>Mean particle size<br/>when redispersed</i> |
|--------------|--------------------------------|---|--|
| 1            | 1:1                            | 200nm   | 210nm  |
| 2            | 2:1                            | 200nm   | 245nm  |
| 3            | 1:0                            | 200nm   | 304nm  |
| 4*           | 1:0                            | 200nm   | 393nm  |

\*Spray coated without additional stabilizers

### 4.3 Processability for different coating substrates

Mannitol and sucrose are the most common used coating substrates in spray- and freeze drying of nanoparticles [4]. Sucrose is the coating substrate used in three nanoproducts on the market namely, EMEND<sup>®</sup>, Rapamune<sup>®</sup> and TriCor<sup>®</sup> while Triglide<sup>™</sup> uses Mannitol (appendix B).

The spray coating tests were carried out based on the sugars glass transition temperatures, where trehalose ought to have the best properties of the sugars to provide optimum processability due to its high T<sub>g</sub>. Initially, sugars of known T<sub>g</sub> were spray coated on MCC cores at a ratio of 1:1 with the API. Additional stabilizers were added together with the sugar to a total concentration of 3.3% (w/w) PVP K30 and 0.14% (w/w) AOT. An experiment without sugar, where the hydrophilic stabilizer PVP K30 could act as the coating substrate was also evaluated, giving a good spray rate due to its non-sticky material characteristics. It was later shown in the redispersion test that PVP K30 did not redisperse and thus did not release enough drug particles.

Aerosil 200<sup>®</sup> which is nanometersized SiO<sub>2</sub> was evaluated because of its antiplasticizing effect and earlier works [18]. It has also been shown that it can be used as a coating substrate as well [31]. In these experiments Aerosil 200<sup>®</sup> was used as an antiplasticizer and not as the coating substrate. The SiO<sub>2</sub> unfortunately had the unwanted attribute to clog the tube in the pump.

Talc was evaluated because of its anticaking abilities to make the process less sticky with an excipient widely used in pharmaceuticals and in the food industry. It was possible to increase the spray rate moderately with a 1:1 ratio between the sugar and the talc before agglomeration appeared in the bed. A trial with trehalose and a mixture of SiO<sub>2</sub> and talc to a ratio of 2:1:1 was also evaluated but with the same results as for the SiO<sub>2</sub> trial, namely clogging of the pump tube.

One trial was made without presetting the dew point temperature, thus giving a process with more moisture. This was shown to have no effect either on the spray rate or the yields. The moisture content probably had to be increased further before results in terms of stickiness could be shown in the fluidized bed.

Spray rates and the product- and coating yields are summarized in table 4.3 and the calculations of the yields and the Tg of the sugars used are found in appendix B.

The overall results showed a correlation between Tg and processability for the saccharides and disaccharides, where a higher Tg of the sugar provided a more efficient process (see appendix B). The spray rate, which determines the processability, was however not nearly high enough to provide an acceptable process. Trehalose and lactose gave a spray rate of 0.8 and 0.6 g/min respectively while the bed collapsed for sucrose, glucose and fructose. This corresponds well to their Tg where the saccharides have the lowest glass transition temperatures and sucrose has the lowest Tg of the disaccharides. The sugar alcohols and PVP K30 as coating substrates gave an exceptionally good process with no visual agglomeration tendencies. The product yield was overall good for all excipients and the coating yield was also evaluated with good results (see table 4.3).

**Table 4.3.** Results from spray coating of different coating substrates and excipients.

| <i>Coating substrate</i>                 | <i>Spray rate<br/>[g/min]</i> | <i>Product yield<br/>[%]</i> | <i>Coating yield<br/>[%]</i> |
|--|-------------------------------|------------------------------|------------------------------|
| Trehalose                                | 0.8                           | 89.6                         | 80.9                         |
| Lactose                                  | 0.6                           | 90.2                         | 81.3                         |
| Sucrose                                  | n.a                           | n.a                          | n.a*                         |
| Glucose                                  | n.a                           | n.a                          | n.a*                         |
| Fructose                                 | n.a                           | n.a                          | n.a*                         |
| Mannitol                                 | 1.2                           | 92.6                         | 85.9                         |
| Myo-Inositol                             | 1.6                           | 86.6                         | 74.5                         |
| PVP K30                                  | 2.0                           | n.a                          | n.a**                        |
| Trehalose, SiO <sub>2</sub> , talc 2:1:1 | 1.7                           | n.a                          | n.a                          |
| Trehalose & talc 1:1                     | 1.2                           | 97.3                         | 95.6                         |
| Trehalose at 20° and RH 40%              | 0.8                           | 89.5                         | 80.0                         |

\*Bed collapsed

\*\*Not enough particles released from pellets to scatter the light

#### 4.4 Mean particle size of redispersed nanoparticles

One of the main requirements in this thesis was that the drug particles redispersed rapidly from the coating substrate when in contact with water or gastrointestinal fluids. The particles should redisperse from the coated pellets in the same particle size region as the milled batches before the spray coating. The results showed that the disaccharides trehalose and lactose were the only coating substrates that efficiently prevented agglomeration of the API nanoparticles. Mannitol and myo-inositol probably crystallizes during the spray coating process and are thus incapable of preventing agglomeration of the nanoparticles. This hypothesis led to Raman spectroscopy evaluations to determine if the disaccharides were in an amorphous form after spray coating and if the sugar

alcohols actually crystallized during the coating process. Sucrose would probably have prevented agglomeration if the bed had not collapsed at the set process parameters, since it is also a disaccharide and has been used in formulations for nanoproducts on the market (see appendix B).

The mean particle size of the redispersed pellets is shown in table 4.4. It was shown that the coating substrates which had insufficient processability (spray rate < 0.8 g/min) prevented agglomeration while the coating substrates which had sufficient processability (spray rate > 0.8 g/min) did not prevent agglomeration of the API nanoparticles.

It was not possible to determine the mean particle size of the API from PVP K30 as the coating substrate after 30 minutes in water since there was not enough suspended particles to scatter the light. This could be an indication that the coating substrate did not redisperse fast enough to release the nanoparticles.

**Table 4.4.** Mean particle size before and after the spray coating process.

| <i>Coating substrate</i>                 | <i>Mean particle size before spray coating [nm]</i> | <i>Mean particle size after spray coating [nm]</i> |
|--|---|--|
| Trehalose                                | 180   | 210  |
| Lactose                                  | 180   | 212  |
| Sucrose                                  | 180   | n.a*   |
| Glucose                                  | 180   | n.a*   |
| Fructose                                 | 180   | n.a*   |
| Mannitol                                 | 150   | 340  |
| Myo-Inositol                             | 150   | 240  |
| PVP K30                                  | 150   | n.a**  |
| Trehalose, SiO <sub>2</sub> , talc 2:1:1 | 150   | 310  |
| Trehalose, talc 1:1                      | 150   | 270  |
| Trehalose at 20° at 40% RH               | 180   | 210  |
| EMEND <sup>®</sup>                       | n.a   | 280  |

\*Bed collapsed

\*\*Not enough particles released from pellets to scatter the light

#### 4.5 Amorphous or crystalline coating substrate

It has been shown that trehalose has an amorphous form after spray drying while mannitol crystallizes in another spray drying application [38]. Cores coated with API and trehalose and cores coated with API and mannitol were examined with Raman spectroscopy to evaluate if any phase transitions had occurred for the coating substrates during the spray coating process.

The hypothesis was that when the sugars were coated, they must dry in an amorphous form so that the nanoparticles can be embedded into the coating substrate and thus

agglomeration is prevented. The redispersion performance would also be further increased when the sugar was in its amorphous form.

Mannitol was shown to undergo a phase transition from its pure crystalline  $\beta$ -form (see fig. 4.1, blue line) to another crystalline  $\alpha$ -form indicated by the peak at approximately  $886\text{ cm}^{-1}$  which appears for the processed mannitol but not for the pure form. When coating the API with mannitol (see fig. 4.1, red line) it appears that mannitol forms a mixture of the crystalline  $\alpha$ - and  $\beta$ -form [39]. This crystalline form of mannitol can possibly explain why the sugar alcohols were incapable of preventing agglomeration of the drug nanoparticles when processed.

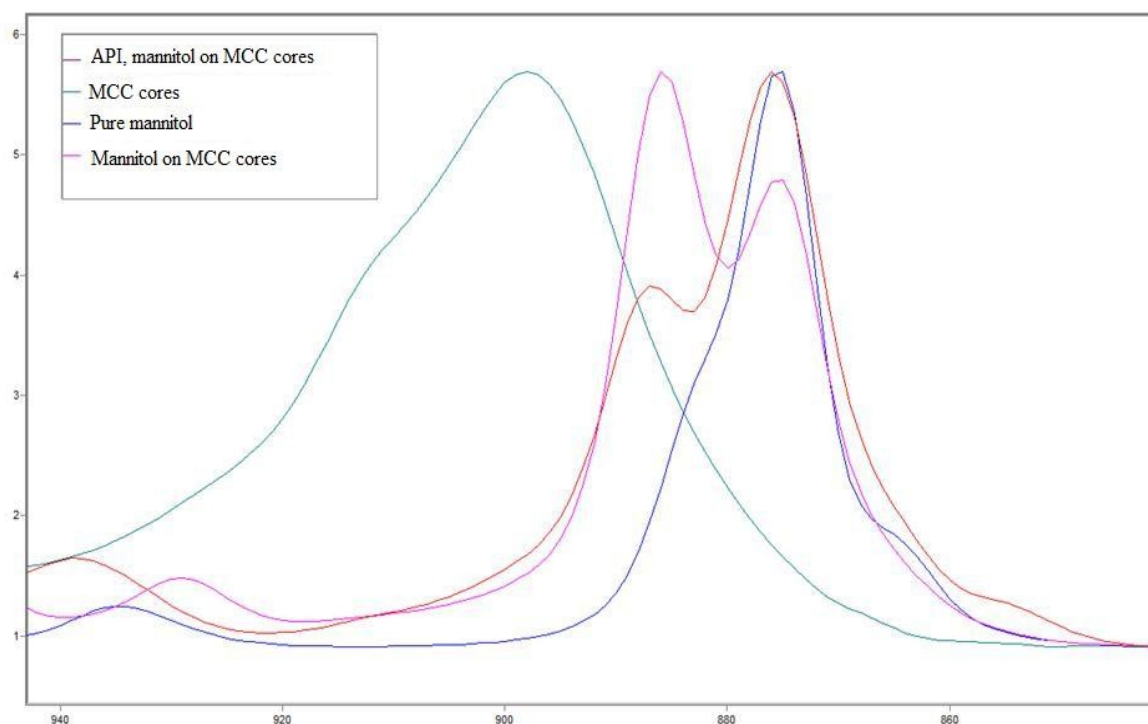


**Figure 4.1.** Raman spectra showing crystalline transitions of mannitol.

Trehalose gave a good indication to be in the amorphous form after the spray coating process. The reference sample was in a dihydrate form (see fig. 4.2, green line) and there was no indication of the spray coated trehalose to still be in the dihydrate form or any other crystalline form, thus the spray coated trehalose was most likely amorphous after spray coating. The crystalline forms of trehalose are indicated by sharp well resolved peaks while the amorphous form shows more broad peaks (see fig. 4.2) [40].

These phase transitions can be an explanation why the sugar alcohols mannitol and myo-inositol are incapable of preventing agglomeration of the nanoparticles. An additional Raman spectrum for trehalose can be viewed in appendix B.

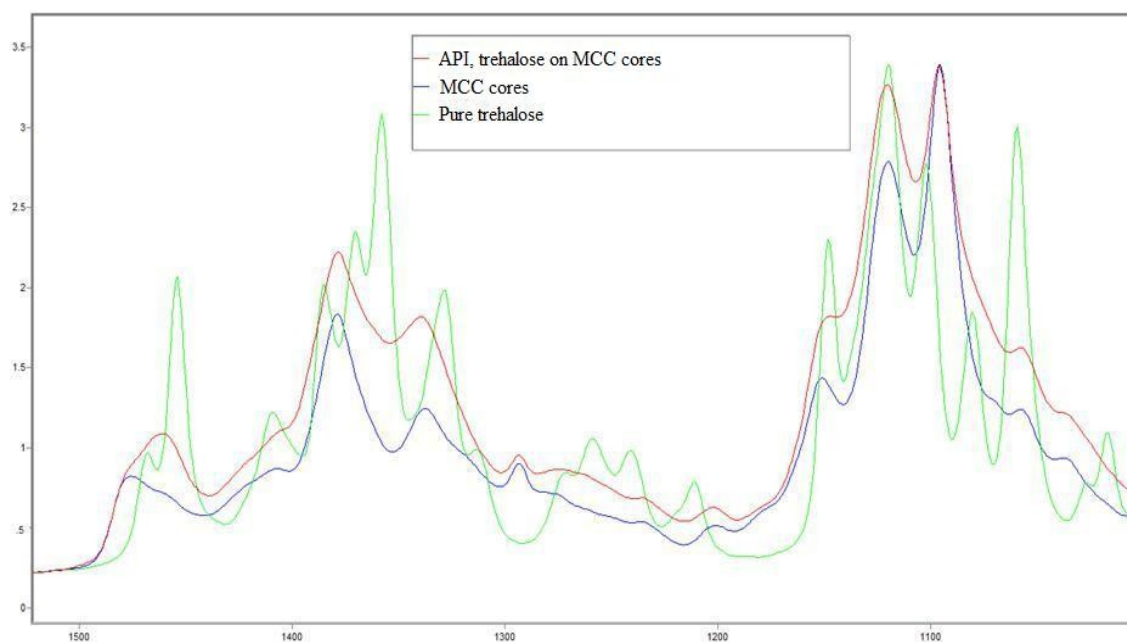


**Figure 4.2.** Raman spectra showing phase transition of trehalose.

#### 4.6 Composition and drug load of the nanosuspensions

The disaccharides that prevented agglomeration gave insufficient spray rates and thus poor processability and the sugar alcohols which provided better processability did not prevent agglomeration of the nanoparticles. Since this was shown and additional excipients added were unable to provide sufficient processability, new batches of higher API concentrations were milled to obtain a nanosuspension with less water content.

Two 30% API nanosuspensions were milled, which provided nanosuspensions with water content of 40% after the coating substrate had been added, if the stabilizers were neglected. This can be compared with the premilled 10% API nanosuspensions with water content of 80% after adding the coating substrate at a ratio of 1:1.

The processability was however not improved compared to the 10% API nanosuspension. The 30% API nanosuspension with trehalose gave redispersed particles in the same range as the 10% nanosuspension. Good product- and coating yields were obtained for both compositions, however the processability was not improved. Although, since the spray rate was equal for both compositions, the 30% API nanosuspension provided three times higher API amounts applied to the pellets within the same process time. This enabled a high drug load when filling the capsules with pellets and thus more opportunities of filling smaller capsules to provide a variety of doses for different purposes. For capsule size 1, a maximum dose of 110 mg could be filled (see table 4.5).

**Table 4.5.** Drug load and dose in capsule size 1.

| <i>Drug load</i> | <i>Dose in capsule 1</i> |
|------------------|--------------------------|
| 324 mg/g         | 110mg                    |

#### 4.7 Determination of coating layer thickness

The amount of applied coating on the cores and the mean diameter volume was determined with beadcheck analyzer and the software Pharmavision 830. Comparison of coating thickness was made with compositions of 10, 20 and 30% API with trehalose. It was shown that the thickness of the coat increased significantly in relation to the size of the cores with increased amount of drug and sugar. The amount of coat applied can be found in table 4.6 and figure 4.3.

**Table 4.6.** Amount of applied coat.

|                     | <i>D</i> [4,3] | <i>Applied coat based on volume [%]</i> |
|---------------------|----------------|---|
| MCC cores           | 452.8 $\mu$ m  | 0                                       |
| 10% API & trehalose | 539.0 $\mu$ m  | 29                                      |
| 20% API & trehalose | 584.8 $\mu$ m  | 40                                      |
| 30% API & trehalose | 660.4 $\mu$ m  | 53                                      |

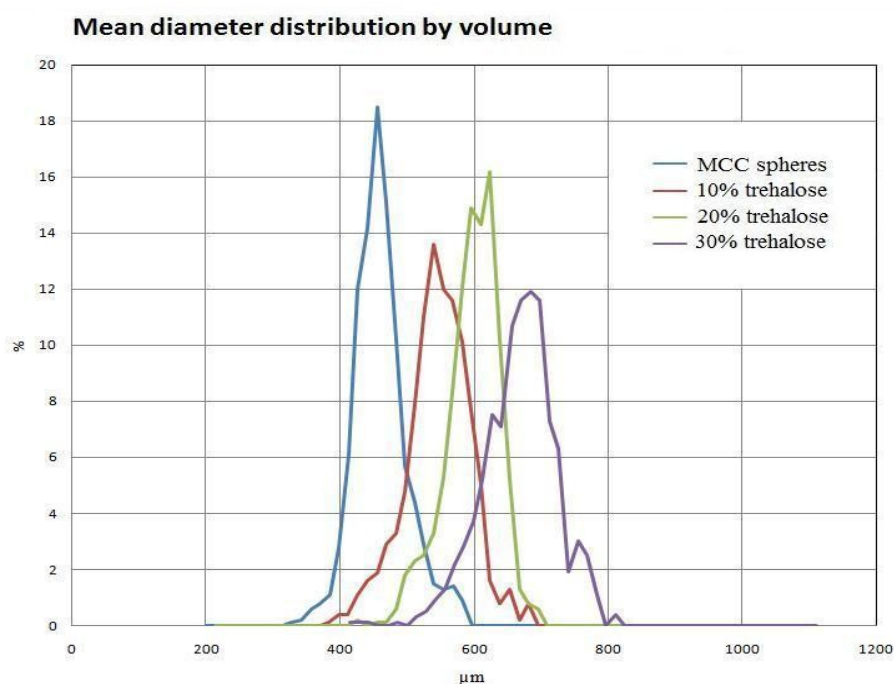


**Figure 4.3.** Mean diameter distribution by volume curve for different compositions of API and trehalose.

#### 4.8 Optimization of the process parameters

The processability of the coating substrates could not be improved by adjusting the composition and excipients of the crystalline nanosuspensions. Thus, in contrast to the original scope of this thesis process parameters had to be optimized. The process parameters of the fluidized bed were probably of higher importance when spraying a sticky substance such as sugars.

#### 4.9 Coating with increased airflow and increased temperature out

The airflow used in the lab fluid bed coater was preset to 10 Nm<sup>3</sup>/h. The maximum airflow which can be achieved in the lab fluid bed coater is 29 Nm<sup>3</sup>/h. Such airflow would theoretically allow a spray rate of 6.25 g/min. The risk which was anticipated with increased airflow was that the droplets could dry before hitting the MCC cores and thus provide poor product- and coating yields. A higher airflow rate would provide more movement in the bed and the risk of cores getting stuck in the upper filter would also increase.

**Table 4.7.** *Process parameters after optimization.*

| <i>Parameters</i>     | <i>Lab fluid bed coater</i> | <i>Optimized setpoints</i> |
|-----------------------|-----------------------------|----------------------------|
| T <sub>in</sub>       | 75°                         | 75°                        |
| T <sub>out</sub>      | 42-49°                      | 65°                        |
| Dew point temperature | 4°                          | 4°                         |
| Inlet air flow        | 10 Nm <sup>3</sup> /h       | 20-29.5 Nm <sup>3</sup> /h |
| Atomizer air flow     | 1 Nm <sup>3</sup> /h        | 1 Nm <sup>3</sup> /h       |
| Spray rate            | 0.8-1.0 g/min               | 0.5-6.25 g/min             |

The airflow at the start of the optimized coating process was set to 20 Nm<sup>3</sup>/h with a spray rate of approximately 0.5 g/min. The airflow was then increased with spray rate depending on how the bed appeared in relation to the agglomeration tendency. T<sub>out</sub> was increased a few degrees due to the increased airflow, but to further increase the exhaust air temperature the equipment was insulated and a T<sub>out</sub> of approximately 65° was achieved (see figure 4.4).



**Figure 4.4.** *The lab fluid bed coater with insulation to obtain a higher  $T_{out}$ .*

Increased exhaust air temperature provides a faster evaporation of the water but it can also give a more sticky process. An increased exhaust air temperature would on the other hand decrease the relative humidity and thus give a more dry process. The temperature and spray rate range where it is possible to spray sugar is limited and can be explained by figure 4.5, where a functional range is found at a medium spray rate and at a medium  $T_{out}$  where the two lines cross each other. The point where the two lines cross should be as low as possible for best yields and minimum agglomeration. The new process parameter was anticipated to provide spray drying and thus poor yields.

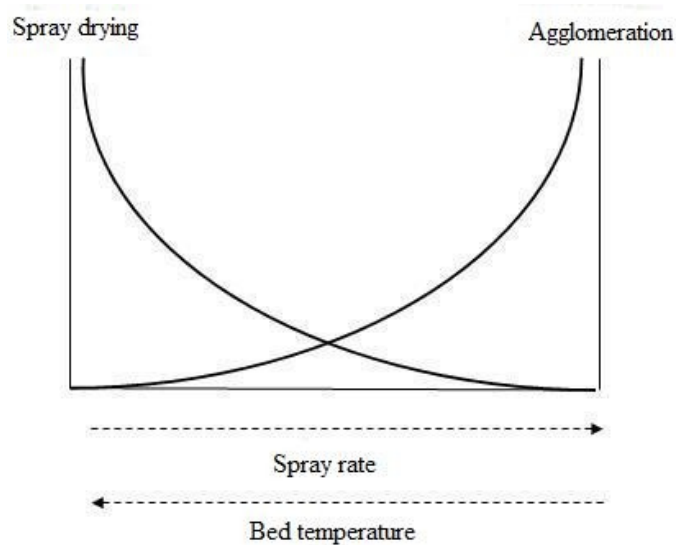


**Figure 4.5.** *Processability region for sugars in fluidized beds with focus on temperature and spray rate.*

The processability was shown to be significantly better for all compositions of trehalose with the increased airflow (see table 4.8). Coating of 20% sucrose with a ratio of 1:1 to API was also conducted with good results compared to the trials with lower airflow where the fluidized bed collapsed. There were some agglomeration tendencies at 2.5 g/min but the process was overall sufficient.

The product yield was excellent for the 10% API pellets where yields over 92% were obtained. The 20% and 30% trehalose pellets had a yield of 82-83% while the 20% sucrose pellet had a yield of 77.9% (see table 4.8). This can be compared with the results in table 4.3 where the yields for trehalose and lactose were approximately 90%.

The product yields were higher for processing lower amounts of API in the nanosuspensions, especially for lower exhaust air temperature ( $T_{out}$ ) (see table 4.8).

An additional trial was made without adding stabilizers to a 30% API nanosuspension prior the coating. This trial provided a very poor yield and moderate spray rate (see table 4.8). The low yield and agglomeration tendencies of the pellets without additional stabilizers can perhaps be explained by the PVP K30s ability to increase the  $T_g$  of trehalose and sucrose [41].

The sugars ability to prevent agglomeration of the API nanoparticles at high airflows was effective for the 20% and 30% trehalose as well as for the 20% sucrose composition, leading to the same mean particle size before and after the spray coating. The 10% trehalose compositions did not prevent agglomeration of the nanoparticles that efficiently upon redispersion, thus the mean particle size was increased. However, an acceptable mean particle size was obtained for all trials.

The processability was overall significantly better with increased airflow at 29 Nm<sup>3</sup>/h for all coating processes. The spray rate was increased from 0.6-0.8 g/min to almost 4 g/min for trehalose while sucrose gave a spray rate of 2.7 g/min, which was impossible to process with lower airflows. These successful results indicated that a scale up of the process could now be considered.

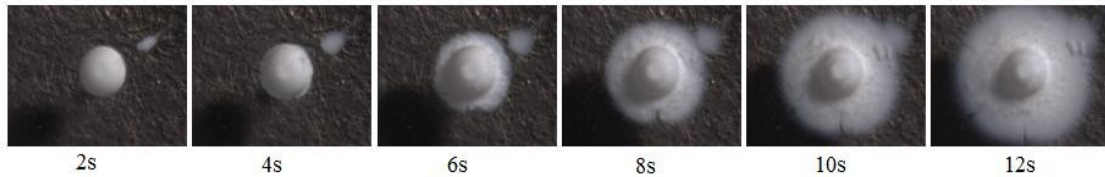
**Table 4.8.** *Spray rate and product yield with adjusted airflow to 29 Nm<sup>3</sup>/h.*

| <b><i>Sugar<br/>(1:1 ratio<br/>with API)</i></b> | <b><i>T<sub>out</sub><br/>[°C]</i></b> | <b><i>Spray<br/>rate<br/>[g/min]</i></b> | <b><i>Agglomeration<br/>tendency</i></b> | <b><i>Product<br/>yield<br/>[%]</i></b> | <b><i>D[4,3]<br/>before<br/>[nm]</i></b> | <b><i>D[4,3]<br/>after<br/>[nm]</i></b> |
|--|--|--|--|---|--|---|
| 20% sucrose                                      | 65                                     | 2.7                                      | yes                                      | 77.9                                    | 285                                      | 285                                     |
| 30% trehalose                                    | 65                                     | 3.7                                      | yes                                      | 82.0                                    | 245                                      | 242                                     |
| 10% trehalose                                    | 55                                     | 3.0                                      | no                                       | 99.8                                    | 150                                      | 254                                     |
| 10% trehalose                                    | 65                                     | 3.0                                      | no                                       | 92.0                                    | 150                                      | 221                                     |
| 20% trehalose                                    | 65                                     | 4.0                                      | no                                       | 83.0                                    | 285                                      | 285                                     |
| 30% trehalose<br>No extra stab.                  | 55                                     | 2.5                                      | yes                                      | 68.1                                    | 285                                      | 285                                     |

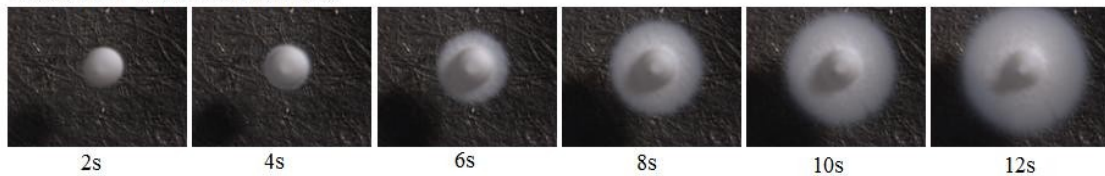
#### 4.10 Visual redispersion with light microscopy

Using light microscopy, the rapid redispersion of the nanoparticles, could be visualized. Pellets manufactured in the lab fluid bed coater released its nanoparticles almost immediately (after 6 seconds) when in contact with the fluid. There was no difference in the redispersion time for the Felodipine pellets (30% respectively 20%) with respect to the sugars (trehalose respectively sucrose) according to figure 4.6. But there was a significant difference compared to the EMEND<sup>®</sup> pellets with the same sugar (see fig.4.6).

30% API with 30% trehalose



20% API with 20% sucrose



EMEND (20%API with 20% sucrose)



**Figure 4.6.** Images showing the redispersion of the sugar with the drug nanoparticles. The same magnification is used in all images.

It was also confirmed that PVP K30 did not dissolve fast enough to be used as a coating substrate for immediate release pellets (see fig. 4.7). There were no changes in the shape of the pellet after 30 minutes. The redispersion profiles of 10% API with trehalose and 10% API with mannitol are shown in appendix B, them being very similar to the 30% API with trehalose and 20% API with sucrose seen in figure 4.6.

10% API with PVP K30 as matrix former

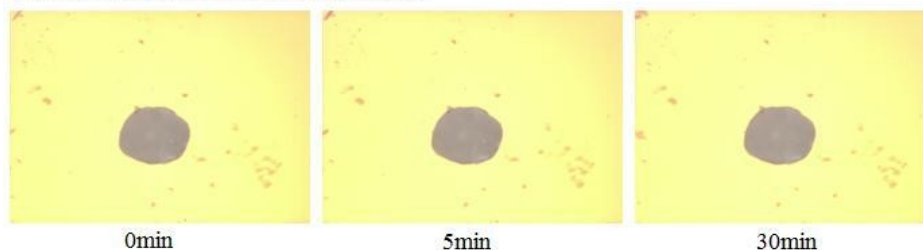


**Figure 4.7.** Pellets coated with PVP K30 as coating substrate.

#### 4.11 Scale up

An optimization of the lab fluid bed coater process could be valuable before scaling up but since the geometrical parameters change significantly and there was no possibility of presetting the dew point temperature in the larger fluidized bed which was available at AstraZeneca, it was decided that a smaller scale up would be more interesting.

The air distributor plate of Gandalf 3 has a diameter of 4 inch and the inlet temperature was set to 80° while the temperature out was held at approximately 70°. The airflow was set to 55 Nm<sup>3</sup>/h in the beginning of the coating process and then increased in relation to the spray rate to the maximum airflow of 60 Nm<sup>3</sup>/h. A spray rate of at least 8 g/min was expected since the airflow was doubled, according to equation 3.3 (see appendix B for calculation). The processability was however shown to be less successful than anticipated with a spray rate of only 2.5 g/min before agglomeration started to occur in the bed. Nanosuspensions with compositions of 10% and 30% API and trehalose were processed.

The airflow in the Gandalf 3 fluidized bed should be doubled to get a similar flow over the plate as the successful coating process in the lab fluid bed coater. In conclusion, the airflow in Gandalf 3 limits the process. This is shown in table 4.9 below and calculations of the areas and spray rates are found in appendix B.

**Table 4.9.** *Airflow over the distributor plate for lab fluid bed coater and Gandalf 3.*

|  | <b>Lab fluid bed coater</b> | <b>Gandalf 3</b> | <b>Gandalf 3 required setpoints</b> |
|--|-----------------------------|------------------|-------------------------------------|
| Air distributor plate area [m <sup>2</sup> ] | 0.0020                      | 0.0081           | 0.0081                              |
| Airflow [Nm <sup>3</sup> /h]                 | 29                          | 60               | 116                                 |
| Flow over plate [m/s]                        | 4.03                        | 2.06             | 3.98                                |

When looking at the airflow parameter with the  $(4/2)^2 = 4$  value, this had good correlation with the flow over the air distributor plate since 29 Nm<sup>3</sup>/h x 4 = 116 Nm<sup>3</sup>/h. The airflow of Gandalf 3 should be doubled to get processability corresponding to the lab fluid bed coater.

Another parameter that could be decisive for the processability of the scale up trial was the moisture content in the bed and the ability of the heated air to evaporate the water content with the used process parameters. Moisture was brought into the bed from three sources, namely from the suspension, the moisture in the air from the inlet airflow and from the moisture in the atomizer flow. The water content per kilogram for the preset dew point temperature can be read out from a mollierdiagram (see appendix C). In the case of Gandalf 3, the moisture per kilogram can also be read out from a mollierdiagram from the room temperature (20°) and its relative humidity (40%). The dew point temperature at 4° for the lab fluid bed coater provided a moisture value of 5 g H<sub>2</sub>O/kg air. Gandalf 3 provided a moisture value of 6 g H<sub>2</sub>O/kg air (see mollierdiagram in

appendix C). The moisture content in the suspensions is expressed as g/h as well as the airflow moisture content. The values are summarized in table 4.10.

The moisture content in the airflow is based on the STP (Standard Temperature and Pressure at 0° and 0.986atm) density of 1.29 kg/m<sup>3</sup>. Calculations of the moisture and the drying ability in the airflows are shown in appendix C. The moisture per kilogram air and relative humidities are shown in the mollierdiagram in appendix C.

**Table 4.10.** *Moisture contents and drying capacity values of the processes.*

|                                    | <i>Lab fluid bed coater</i>   | <i>Gandalf 3</i>               |
|------------------------------------|-------------------------------|--------------------------------|
| Moisture from DP and room humidity | 0.005 kg/kg                   | 0.006 kg/kg                    |
| Suspension                         | 96 g/h                        | 60 g/h                         |
| Airflow                            | 187 g/h                       | 464 g/h                        |
| Atomizerflow                       | 0.6 g/h                       | 0.7 g/h                        |
| Total moisture into bed            | 284 g/h                       | 525 g/h                        |
| Relative humidity                  | 4%                            | 3%                             |
| Drying capacity                    | 2.5g H <sub>2</sub> O /kg air | 0.8 g H <sub>2</sub> O /kg air |

The relative humidities were similar and the process was very dry in the fluidized beds with the purpose to decrease the sticky behavior of the sugar used.

The drying capacity for Gandalf 3 was shown to be exceptionally low in comparison to the lab fluid bed coater. When looking at the drying capacities and the flow over the distributor plates it is more obvious that agglomeration started at 2.5 g/min.

#### **4.12 Quality of the pellets uniformity**

The coating quality was inspected more thoroughly with SEM, showing the smoothness of the coat and an estimation of the porosity of the coat from the cleaved pellets. It was shown that the coating was more uniform and smooth when processed in the lab fluid bed coater than in Gandalf 3. The product EMEND<sup>®</sup> from Merck had a rough surface (see fig. 4.8). The same characteristics could be seen when comparing the 30% trehalose trials in the lab fluid bed coater and Gandalf 3 (see appendix C). Cracks were seen in the coat for EMEND<sup>®</sup> and from the lab fluid bed coater process of 30% trehalose, although the cracks from the lab fluid bed coater process were significantly smaller.

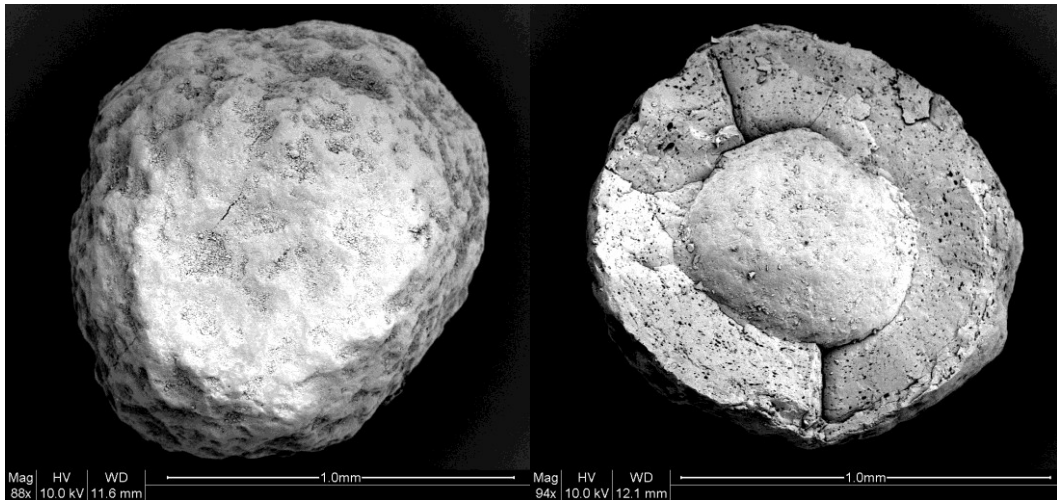


**Figure 4.8.** SEM images of EMEND<sup>®</sup> showing the coatings and cracks from the cleaved pellet. The MCC core can be seen in the middle of the cleaved pellet.

The coating of 20% sucrose in the lab fluid bed coater equipment showed the most uniform coat with no cracks (figure 4.9). It was shown that the smoothness of the pellets decreased with increasing airflow, probably due to more collisions between the pellets in the bed when elevated. The cracks are probably not important for immediate release products. The cracks can though become a robustness problem if further functional coatings should be applied.

The quality of the coating was best for the lab fluid bed coater process in terms of smoothness and uniformity of the coat. Large cracks were observed in the coating for EMEND<sup>®</sup> and smaller cracks were seen in the lab fluid bed coater process for trehalose. The cracks were eliminated in Gandalf 3 but the coat had a rough surface, probably due to the higher airflow.

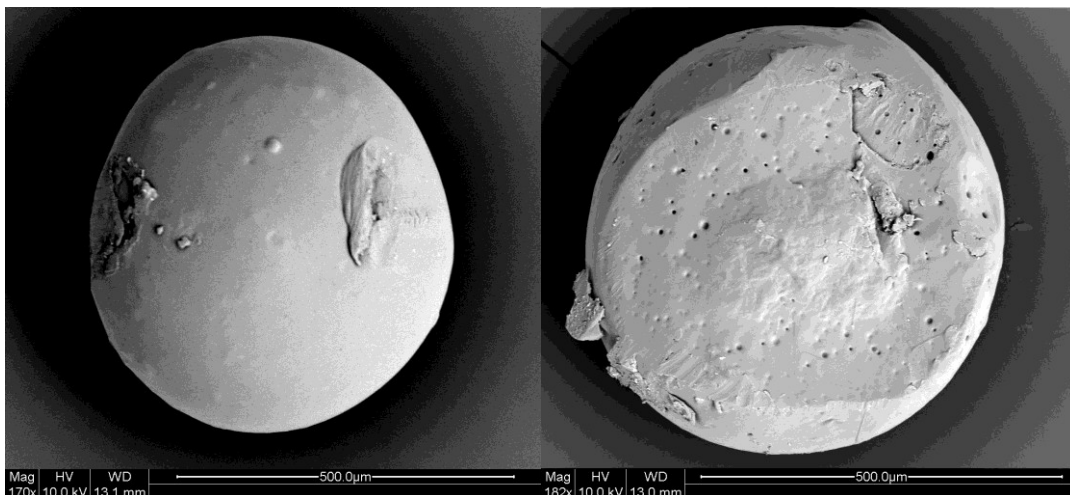


**Figure 4.9.** SEM images of 20% sucrose in the lab fluid bed coater showing a very uniform coat with no visual cracks.

## 5 Conclusions

The disaccharides trehalose, sucrose and lactose were shown to prevent agglomeration of the crystalline nanoparticles most efficiently. Trehalose with a T<sub>g</sub> of 107° gave best processability of the disaccharides followed by lactose with a T<sub>g</sub> of 101° and then sucrose with a T<sub>g</sub> of 60° indicating that the stickiness is determined mostly by the sugars T<sub>g</sub>. Mannitol and myo-inositol were unable to prevent agglomeration, this was probably due to the crystallization of the sugars during the spray coating process while the disaccharides were in an amorphous form after spray coating. The amorphous form was probably able to embed the nanoparticles upon drying more efficiently than the crystalline form.

A ratio of 1:1 between the sugar and the API was shown to stabilize the nanoparticles most efficiently.

The composition of the crystalline nanosuspensions were not a critical parameter though it was notable that a 30% API crystalline nanosuspension could be prepared by wet milling technique for the API, Felodipine leading to an enhanced drug load. The best yields were though obtained for the 10% API nanosuspensions.

The main parameter affecting the processability was the inlet airflow. The inlet airflow was maximized in the lab fluid bed coater to obtain a process with sufficient spray rate. Gandalf 3 was limited by its airflow rate which should be doubled to obtain sufficient flow over the distributor plate. T<sub>out</sub> was not a crucial parameter but the best yields were obtained at a temperature out of approximately 55°.

Adding additional stabilizers prior the spray coating seemed to improve the processability and the yields.

By calculating the moisture content, relative humidity and drying capacities of the inlet and exhaust air, one can predict the processability e.g. spray rate of sugars in the process.



## **6 Future work**

Trehalose is in an amorphous form after spray drying and thus more physically unstable. A stability measurement should be done to determine when the amorphous trehalose crystallizes upon storage. Light scattering measurements showing if the crystallized coating substrate could prevent agglomeration of the nanoparticles would be interesting. The redispersion rate could be evaluated with light microscopy.



## 7 References

- [1]. Rabinow, B.E. (2004). *Nanosuspensions in drug delivery*. Drug disc. Nature reviews, vol. 3, ss. 785-796.
- [2]. Aulton, M.E. (red.) (2002). *Pharmaceutics - the science of dosage form design*, 2<sup>nd</sup> ed. Edinburgh: Churchill Livingstone.
- [3]. Chaubal, M.V. & Popescu, C. (2008). Conversion of Nanosuspensions into Dry Powders by Spray Drying: A Case Study. *Pharma. Res.* Vol. 25, No. 10.
- [4]. Van Eerdeburgh, B., Van den Mooter, G. & Augustijns, P. (2008). *Top-down production of drug nanocrystals: Nanosuspension stabilization, miniturization and transformation into solid products*. *Int. J. of Pharma.* 364, ss. 64-75.
- [5]. Chen, X.D. (2007). *Conformability of the kinetics of the cohesion/stickiness development in amorphous sugar particles to the classical Arrhenius law*. *J. of Food Eng.* 79, ss. 675-680.
- [6]. Guignon, B., Regalado, E., Duquenoy, A. & Dumoulin, E. (2003). *Helping to choose operating parameters for a coating fluid bed process*. *Powder Tech.* Vol. 130, issues 1-3, ss. 193-198.
- [7]. Shelukar, S., Ho, J., Zega, J., Roland, E., Yeh, N., Quiram, D., Nole, A., Katdare, A. & Reynolds, S. (2000). *Identification and characterization of factors controlling tablet coating uniformity in a wurster coating process*. *Powder Tech.* Vol. 110, issues 1-2, ss. 29-36.
- [8]. Nicklasson Björn, I., Folestad, S., Johansson, M. & Josefsson, L. (2002). *Multivariate analysis for product design and control*. *Comp. Aided Chem. Eng.* Vol. 10, ss. 133-138.
- [9]. Visser, M.R., Baert, L., Van't Klooster, G., Schueller, L., Geldof, M., Vanwelkenhuysen, I., De Kock, H., De Meyer, S., Frijlink, H.W., Rosier, J. & Hinrichs, W.L.J. (2010). *Insulin solid dispersion technology to improve the absorption of the BCS Class IV drug TMC240*. *Eur. J. of Pharma. and Biopharma.* 74, ss. 233-238.
- [10]. Chingunpituk, J. (2007). *Nanosuspension Technology for Drug Delivery*. *Walailak J. Sci. & Tech.*; 4(2), ss. 139-153.
- [11]. Kesisoglou, F., Panmai, S. & Wu, Y. (2007). *Nanosizing – Oral formulation development and biopharmaceutical evaluation*. *Adv. Drug. Del. Rev.* 59, ss. 631-644.
- [12]. Möschwitzer, J. & Müller, R.H. (2005). *Spray coated pellets as carrier system for mucoadhesive drug nanocrystals*. *Eur. J. of Pharma. & Biopharma.* 62, ss. 282-287.
- [13]. Mihranyan, A. & Strømme, M. (2007). *Solubility of fractal nanoparticles*. *Surface Science* 601, ss. 315-319.

- [14]. Holmberg, K., Jönsson, B., Kronberg, B. & Lindman, B. (2003). *Surfactants and polymers in aqueous solution* 2<sup>nd</sup> ed. Norfolk: John Wiley & Sons Ltd.
- [15]. Lindfors, L., Skantze, P., Skantze, U., Rasmusson, M., Zackrisson, A. & Olsson, U. (2006). *Amorphous Drug Nanosuspensions. 1. Inhibition of Ostwald Ripening*. *Langmuir*, 22, ss. 906-910.
- [16]. Merisko-Liversidge, E., Liversidge, G.G. & Cooper, E.R. (2003). *Nanosizing: a formulation approach for poorly water-soluble compounds*. *Eur. J. of Pharma. Sc.* 18, ss. 113-120.
- [17]. Ravichandran, R. (2009). *Nanoparticles in drug delivery: Potential Green Nanobiomedicine Applications*. *Int. J. of Green Nanotech.: Biomed.*, 1:2, ss. B108-B130.
- [18]. Hoppu, P. (2008). Characterisation and processing of amorphous binary mixtures with low glass transition temperature. Diss. Faculty of Pharmacy, University of Helsinki, Finland.
- [19]. Savolainen, M. (2008). New Insights into the Amorphous State and Related Solid-State Transformations. Diss. Faculty of Pharmacy, University of Helsinki, Finland.
- [20]. Janssens, S. & Van den Mooter, G. (2009) *Review: physical chemistry of solid dispersions*. *J. of Pharm. and Pharmacol.* 61, ss. 1571-1586.
- [21]. Cowie, J.M.G. & Arrighi, V. (2008). *Polymers: Chemistry and Physics of Modern Materials* 3<sup>rd</sup> ed. Boca Raton: CRC Press.
- [22]. Qiu, Yihong, Chen, Yisheng & Geoff G.Z. (2009) *Developing solid oral dosage forms: pharmaceutical theory and practice*. [Electronic]. 1<sup>st</sup> ed. Amsterdam: Elsevier
- [23]. Vergote, G.J., Vervaet, C., Van Driessche, I., Host, S., De Smedt, S., Demeester, J., Jain, R.A., Ruddy, S. & Remon, J.P. (2001) *An oral controlled release matrix pellet formulation containing nanocrystalline ketoprofen*. *Int. J. of Pharma.* ss. 81-87.
- [24]. Karlsson, S. (2007). *Particle Coating in a Wurster Type Bed*. Diss. Dep. Of Chemical and Biological Engineering, Chalmers Uni. of Tech.: Göteborg.
- [25]. Wurster, D.E. (1959). *Air-Suspension Technique of Coating Drug Particles*. *J. of the Amer. Pharma. Ass.* Vol. XLVIII, no 8, ss. 451-454.
- [26]. Christensen, F.N. & Bertelsen, P. (1997). *Qualitative Description of the Wurster-Based Fluid-Bed Coating Process*. *Drug Dev. and Ind. Pharm.* 23(5), ss. 451-463.
- [27]. Wen, H. & Park, K. (2010). *Oral Controlled Release Formulation Design and Drug Delivery: Theory to Practice*. [Electronic]. Hoboken, New Jersey: John Wiley & Sons.
- [28]. CHEMnetBASE, "Dictionary of drugsinch [Electronic]. Taylor & Francis Group, [2011-04-01].

- [29]. DrugBank. <http://www.drugbank.ca/drugs/DB01023#>, [2011-04-01].
- [30]. Medicines Complete, Pharmaceutical excipients. <http://www.medicinescomplete.com/mc/excipients/current/1001944386.htm>, [2011-04-01].
- [31]. Van Eerdenbrugh, B., Froyen, L., Van Humbeeck, J., Martens, A.J., Augustijns, P. & Van den Mooter, G. (2008). Alternative coating substrates for nanosuspension solidification: Dissolution performance and X-ray microanalysis as an evaluation tool for powder dispersion. *Eur. J. of Pharma. Sc.* 35, ss. 344-353.
- [32]. Drugs@FDA. <http://www.accessdata.fda.gov/scripts/cder/drugsatfda>, [2011-04-13].
- [33]. Simperler, A., Kornherr, A., Chopra, R., Arnaud BoNet, P., Jones, W., Samuel Motherwell, W.D. & Zifferer, G. (2006). Glass Transition temperatures of Glucose, Sucrose and Trehalose: An experimental and in Silico Study. *J. Phys. Chem. B*, Vol. 110, No. 39, ss. 19678-19684.
- [34]. Bouffard, J., Dumont, H., Bertrand, F. & Legros, R. (2007). *Optimization and scale-up of a fluid bed tangential spray rotogranulation process*. *Int. J. of Pharma.* Vol. 335, ss. 54-62.
- [35]. Smart, L.E. & Moore, E.A. (2005). *Solid state chemistry: an introduction*. 3<sup>rd</sup> ed. Boca Raton, Florida: Taylor & Francis
- [36]. Bloomfield, V. A. (2000). *Static and Dynamic Light Scattering from Aggregating Particles*. *Biopolymers*, Vol. 54, 168-172, John Wiley & Sons, Inc.
- [37]. Rao, C.N.R & Gopalakrishnan, J. (1997). *New directions in solid state chemistry*, 2<sup>nd</sup> ed. [Electronic]. Cambridge: Cambridge Univ. Press.
- [38]. Mosén, K. (2003). *Spray drying of particles intended for inhalation – Investigation of significant process variables and product characteristics, with focus on degradation and solid state properties*. Diss. Dept. of Pharma. The Danish University of Pharma. Sci. Copenhagen, Denmark.
- [39]. Xie, Y., Cao, W., Krishnan, S., Lin, H. & Cauchon, N. (2008). *Characterization of Mannitol Polymorphic Forms in Lyophilized Protein Formulations Using a Multivariate Curve Resolution (MCR)-Based Raman Spectroscopic Method*. *Pharma. Res.*, Vol. 25, No. 10, ss. 2292-2301.
- [40]. Chakravarty, P., Bhardwaj, S.P., King, L. & Suryanarayanan, R. (2009). *Monitoring Phase Transformations in Intact Tablets of Trehalose by FT-Raman Spectroscopy*. *AAPS PharmSciTech*, Vol. 10, No. 4, ss. 1420-1426.
- [41]. Zhang, J. & Zografi, G. (2001). *Water Vapor Absorption Into Amorphous Sucrose- Poly(Vinyl Pyrrolidone) and Trehalose-Poly(Vinyl Pyrrolidone) Mixtures*. *J. of Pharma. Sci.*, Vol. 90, NO. 9, ss. 1375-1385.



## Appendix

### A.

#### Myo-Inositol

Sugar alcohol obtained from Sigma-Aldrich Co St. Louis, USA. Chemical formula;  $C_6H_{12}O_6$  which is a sixfold alcohol of cyclohexane. Calculated Tg value of  $221^\circ$ .

#### Fructose

Saccharide, obtained from KEBO Lab Spånga, Sweden. Tg value of approximately  $25^\circ$ .

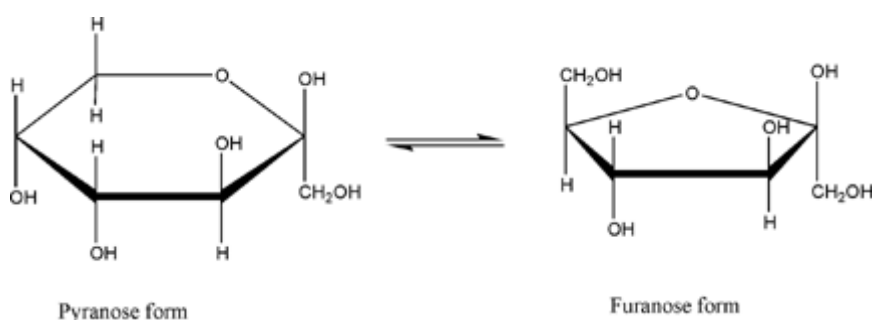


**Figure A.1.** Chemical structure of the pyranose and furanose form of fructose [30].

#### Glucose

Saccharide obtained from KEBO Lab Spånga, Sweden. Tg of approximately  $52^\circ$ . The structure is very similar to that of fructose.

#### Lactose

Disaccharide, obtained from Kerry Bio-Science Michigan, USA. Tg =  $101^\circ$

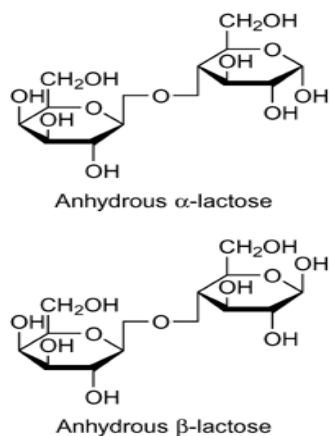


**Figure A.2.** The chemical structure of lactose [30].

**SiO<sub>2</sub> Aerosil 200**

Colloidal silicon dioxide obtained from Evonik Degussa GmbH Hanau-Wolfgang, Germany is water soluble antiplasticizers with primary particles around 15 nm. It works as an adsorbent, anticaking agent, emulsion stabilizer, glidant, suspending agent, tablet disintegrant, thermal stabilizer and viscosity increasing agent.

**Talc**

Talc obtained from RioTinto Colorado, USA is a purified, hydrated magnesium silicate with functionalities as anticaking agent, glidant, diluent for capsules and lubricant and diluents for tablets and capsules.

## B.

### Nanocrystalline API products on the market

**Table B.1.** *Nanocrystalline API products on the market 2011 [4].*

| <i>Product</i>         | <i>FDA approval</i> | <i>Company</i>                  | <i>Manufacturing technique</i>            |
|------------------------|---------------------|---------------------------------|---|
| Rapamune <sup>®</sup>  | 2000                | Wyeth                           | Top-down media milling                    |
| EMEND <sup>®</sup>     | 2003                | Merck                           | Top-down media milling                    |
| TriCor <sup>®</sup>    | 2004                | Abbott                          | Top-down media milling                    |
| MEGACE <sup>®</sup> ES | 2005                | PAR<br>Pharmaceutical           | Top-down media milling                    |
| Triglide <sup>™</sup>  | 2005                | First Horizon<br>Pharmaceutical | Top-down, high pressure<br>homogenization |

### Yield calculations

#### Trehalose

14.52 g solid amount

23.75 g product weight

12.00 g pellet weight

Product yield:  $23.75 \text{ g} / (14.52 \text{ g} + 12.00 \text{ g}) = 0.896$

Coating yield:  $23.75 \text{ g} - 12.00 \text{ g} = 11.75 \text{ g}$

$11.75 \text{ g} / 14.52 = 0.809$

#### Lactose

13.24 g solid amount

22.93 g product weight

12.17 g pellet weight

Product yield:  $22.93 \text{ g} / (13.24 \text{ g} + 12.17 \text{ g}) = 0.902$

Coating yield:  $22.93 \text{ g} - 12.17 \text{ g} = 10.76 \text{ g}$

$10.76 \text{ g} / 13.24 = 0.813$

#### Mannitol

13.44 g solid amount

23.55 g product weight

12.00 g pellet weight

Product yield:  $23.55 \text{ g} / (13.44 \text{ g} + 12.00 \text{ g}) = 0.926$

Coating yield:  $23.55 \text{ g} - 12.00 \text{ g} = 11.55 \text{ g}$

$11.55 \text{ g} / 13.44 = 0.859$

**Myo-Inositol**

13.24 g solid amount  
21.87 g product weight  
12.00 g pellet weight

Product yield:  $21.87 \text{ g} / (13.24 \text{ g} + 12.00 \text{ g}) = 0.866$

Coating yield:  $21.87 \text{ g} - 12.00 \text{ g} = 9.87 \text{ g}$

$9.87 \text{ g} / 13.24 = 0.745$

**Trehalose and talc 1:1**

19.24 g solid amount  
30.44 g product weight  
12.04 g pellet weight

Product yield:  $30.44 \text{ g} / (19.24 \text{ g} + 12.04 \text{ g}) = 0.973$

Coating yield:  $30.44 \text{ g} - 12.04 \text{ g} = 18.4 \text{ g}$

$18.4 \text{ g} / 19.24 = 0.956$

**Trehalose at 20° and 40% room humidity**

13.24 g solid amount  
22.61 g product weight  
12.02 g pellet weight

Product yield:  $22.61 \text{ g} / (13.24 \text{ g} + 12.02 \text{ g}) = 0.895$

Coating yield:  $22.61 \text{ g} - 12.02 \text{ g} = 10.59 \text{ g}$

$10.59 \text{ g} / 13.24 = 0.800$

**Tg of the sugars**

**Table B.2.** *Tg of the sugars used.*

| <i>Sugar</i> | <i>Tg [°C]</i> |
|--------------|----------------|
| Myo-Inositol | 221*           |
| Trehalose    | 107            |
| Lactose      | 101            |
| Mannitol     | 87             |
| Sucrose      | 60             |
| Glucose      | 52             |
| Fructose     | 25             |

\*Calculated value from Watt, S.W., Chisholm, J.A., Jones, W. & Motherwell, S. (2004). *A molecular dynamics simulation of the melting points and glass transition temperatures of myo- and neo-inositol*. J. of Chem. Phys. Vol. 121, No. 19, ss. 9565-9573.

## Raman spectroscopy

The dihydrate bands of trehalose at 2700-3100  $\text{cm}^{-1}$  are not obviously visible which can be an indication that the trehalose is in an amorphous form after spray coating.

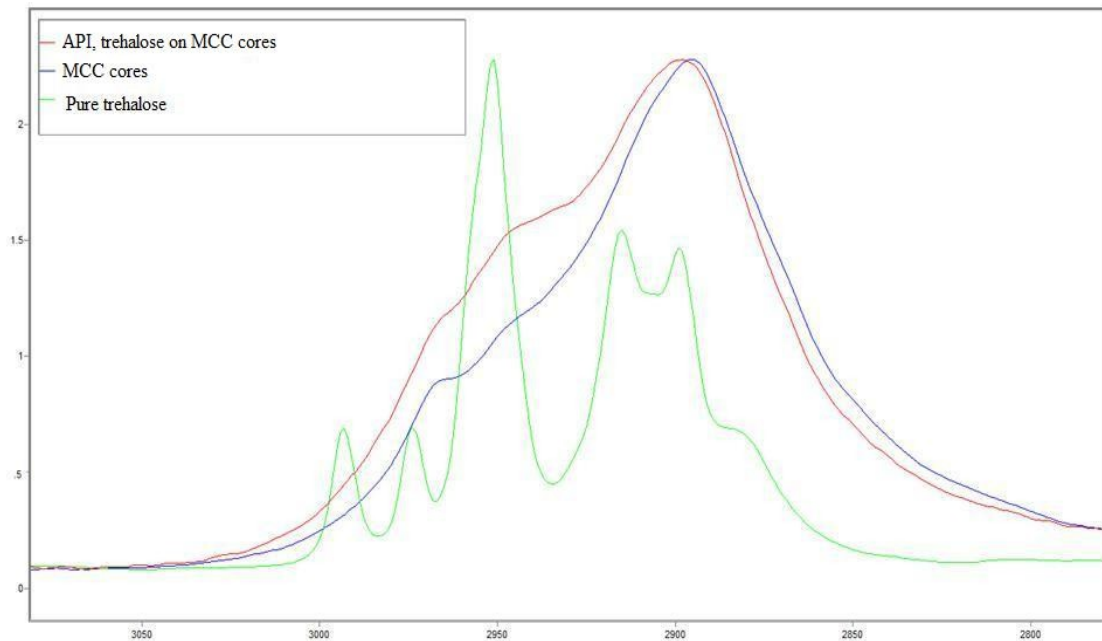


**Figure B.1.** Raman spectroscopy showing phase transition of trehalose.

## Redispersion trehalose and mannitol

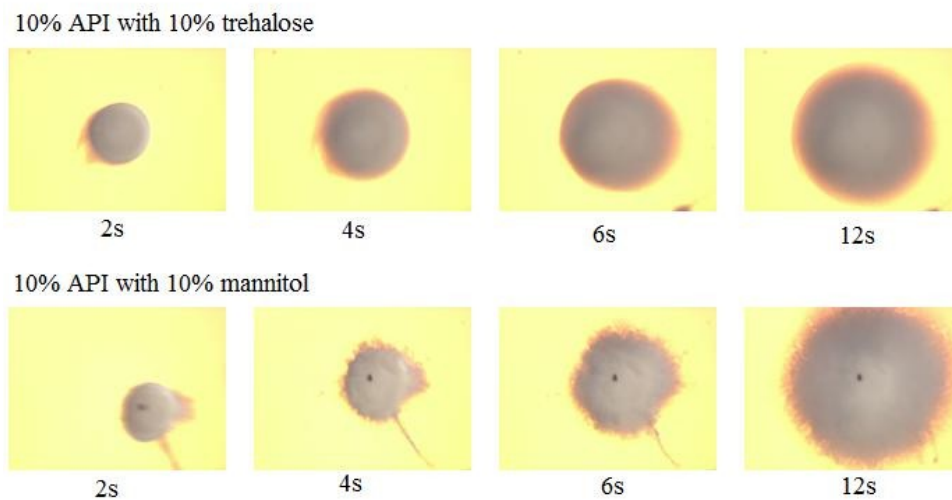


**Figure B.2.** Redispersion of 10% API with trehalose and 10% API with mannitol.

### Scale up calculation

$$S_2 = S_1 \times V_2/V_1, S_2 = 4 \text{ g/min} \times (60 \text{ Nm}^3/\text{h} / 29 \text{ Nm}^3/\text{h}) = 8.276 \text{ g/min}$$

$$A_2 = d^2\pi/4 = (4 \times 2.54 \times 10^{-2})^2\pi/4 = 0.0081 \text{ m}^2$$

$$A_1 = d^2\pi/4 = (2 \times 2.54 \times 10^{-2})^2\pi/4 = 0.0020 \text{ m}^2$$

## C.

### Lab fluid bed coater:

Moisture from 4° dew point temperature and  $T_{in}=75^{\circ}$ . Value from mollierdiagram (0.005 kg H<sub>2</sub>O /kg dry air).

Moisture from suspension:

$$4 \text{ g/min spray rate} \times 0.4 \text{ (water content)} \times 60 = 96 \text{ g/h}$$

Moisture from airflow:

$$29 \text{ Nm}^3/\text{h} \times 1.29 \text{ kg/m}^3 \times 0.005 \text{ kg H}_2\text{O /kg dry air} = 187 \text{ g/h}$$

Moisture from Atomizerflow:

$$1 \text{ Nm}^3/\text{h} * 1.29 \text{ kg/m}^3 \times 0.5 \text{ g/kg} = 0.6 \text{ g/h}$$

Total moisture in:

$$96 \text{ g/h} + 187 \text{ g/h} + 0.6 \text{ g/h} \sim 284 \text{ g/h}$$

Relative humidity:

$$284 \text{ g/h} / (1 \text{ Nm}^3/\text{h} + 29 \text{ Nm}^3/\text{h}) \times 1.29 \text{ kg/m}^3 = 7.3 \text{ g H}_2\text{O /kg air}$$

RH value from mollierdiagram (4%).

### Gandalf 3:

Moisture from 20° room temperature and relative humidity of 40%. Value from mollierdiagram (0.006 kg H<sub>2</sub>O /kg dry air).

Moisture from suspension:

$$2.5 \text{ g/min spray rate} \times 0.4 \text{ (water content)} \times 60 = 60 \text{ g/h}$$

Moisture from airflow:

$$60 \text{ Nm}^3 \times 1.29 \text{ kg/m}^3 \times 0.006 \text{ kg H}_2\text{O /kg dry air} = 464.4 \text{ g/h}$$

Moisture from Atomizerflow:

$$1 \text{ Nm}^3 * 1.29 \text{ kg/m}^3 \times 0.6 \text{ g/kg} = 0.7 \text{ g/h}$$

Total moisture in:

$$60 \text{ g/h} + 464.4 \text{ g/h} + 0.7 \text{ g/h} \sim 525 \text{ g/h}$$

$$464.4 \text{ g/h} / (1 \text{ Nm}^3/\text{h} + 60 \text{ Nm}^3/\text{h}) \times 1.29 \text{ kg/m}^3 = 6.7 \text{ g H}_2\text{O /kg air}$$

RH value from mollierdiagram (3%).

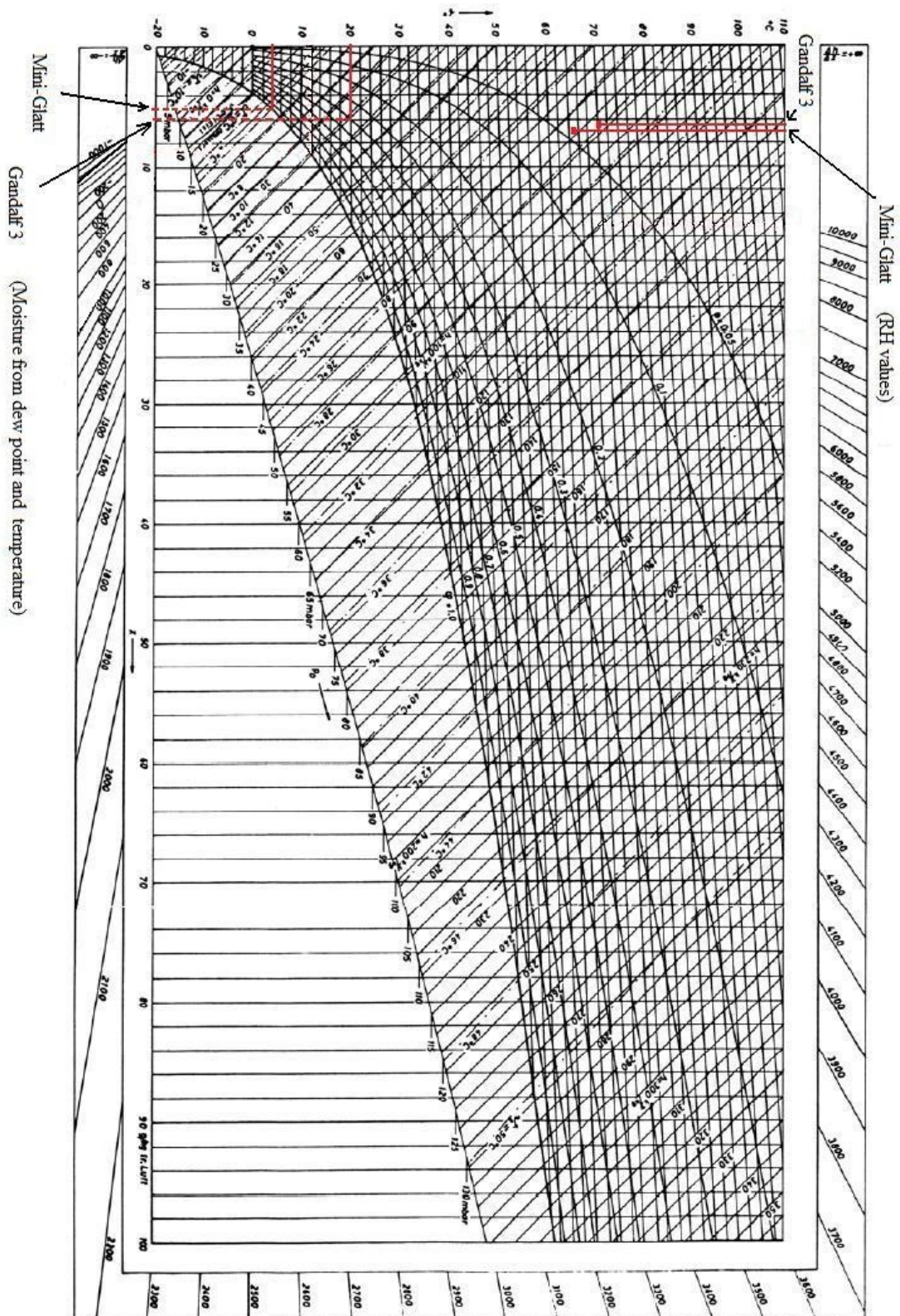
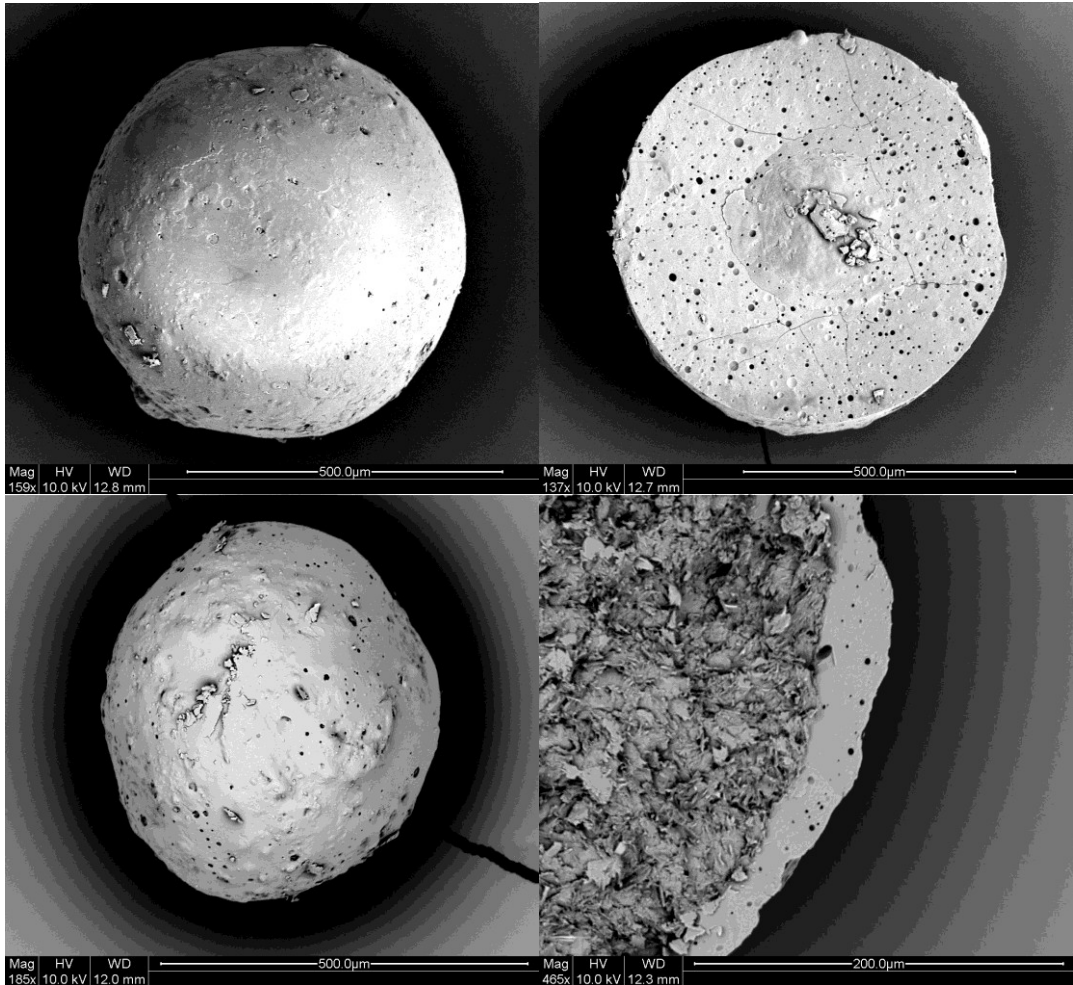


Figure C.1. Mollierdiagram with relative humidities and moisture content for the three fluidized bed processes.



**Figure C.2.** SEM images of 30% API with 30% trehalose. The two pictures on top are the pellets from the process of the lab fluid bed coater while the two bottom pictures are from the Gandalf 3 process. The thickness of the coat in the Gandalf 3 process was low because the process was interrupted due to time limitations.